

Weather, Climatic and Ecological Impacts of Onshore Wind Farms

Liming Zhou^a, Somnath Baidya Roy^b, and Geng Xia^c, ^aDepartment of Atmospheric and Environmental Sciences, University at Albany, State University of New York, Albany, NY, United States; ^bCentre for Atmospheric Sciences, Indian Institute of Technology Delhi, New Delhi, India; ^cNational Wind Technology Center, National Renewable Energy Laboratory (NREL), Golden, CO, United States

© 2020 Elsevier Inc. All rights reserved.

Disclaimer: The *views*, thoughts, and opinions expressed in this book chapter belong solely to the authors and *not* necessarily to the authors' employers and organizations.

1	Introduction	1
2	Wind turbine-atmosphere-surface interactions	2
2.1	Wind turbine wake effects	2
2.2	How wind turbines modify atmosphere-surface interactions	3
2.3	How wind turbines interact with vegetation	3
3	Methods for assessing wind farm impacts	4
3.1	Observational methods	4
3.1.1	Time series analysis	4
3.1.2	Spatial pattern analysis	5
3.1.3	Other observational methods	5
3.2	Modeling methods	5
3.2.1	The enhanced roughness length parameterizations	5
3.2.2	The elevated momentum sink and TKE source parameterizations	6
3.2.3	Other modeling methods	7
4	Weather and climatic impacts of onshore wind farms	8
4.1	Local to regional impacts	8
4.1.1	Impacts on land surface properties	8
4.1.2	Impacts on temperatures	8
4.1.3	Impacts on precipitation	11
4.1.4	Impacts on wind patterns	13
4.2	Large to global scale impacts	14
4.2.1	Impacts on temperature and precipitation	14
4.2.2	Impacts on wind patterns and large-scale circulation	15
5	Ecological impacts of onshore wind farms	16
5.1	Impacts on local vegetation cover	16
5.2	Impacts on crop yields	16
5.3	Impacts on vegetation activity	17
6	Major uncertainties	18
6.1	Observational uncertainties	18
6.2	Modeling uncertainties	18
7	Future work	19
8	Conclusion and discussion	20
8.1	Key summary	20
8.2	Relative to other man-made climate impacts	21
8.3	Final remarks	21
	References	21

1 Introduction

Population, economic activity, and technology are the three most basic drivers of energy demand (Yeager et al., 2012). According to the recent United Nations (UN) report, the world population was about 7.7 billion in 2019 and is expected to reach 9.7 billion in 2050 (UN, 2019). Coupled with advances in technology and growth in population, the global economy has grown exponentially in the past despite some short-term hardships, wars, and other major events (Roser, 2020). In correspondence, global demand for energy has increased rapidly and fossil fuels have been the world's primary energy source feeding the global economic growth over the past century (Yeager et al., 2012). However, fossil fuels are finite and nonrenewable resources and their consumption leads to increasing greenhouse gas (GHG) emissions, particularly carbon dioxide (CO₂), which contribute to global warming, toxic pollution, and other environmental issues. Renewable energy such as the geothermal, biomass, hydroelectric, wind and solar helps to reduce the GHG emissions by burning fossil fuels and ensure sustainable growth in the energy sector (Moomaw et al., 2011; Yeager et al., 2012).

Wind is the movement of air formed as a result of differences in atmospheric pressure. It varies strongly by time, location, and altitude, and is caused by the uneven heating of the atmosphere and surface by the Sun, the irregularities of the Earth's terrain, and the Coriolis forcing of the Earth's rotation (Itskos et al., 2016). This wind flow contains kinetic energy that can be harvested to generate mechanical power or electricity, often called "wind energy" or "wind power." Humans have a long history of harnessing wind energy to generate mechanical power for centuries through wind-powered machines for food production, agriculture and transportation such as sailing, flying a kite, grinding grain, pumping water, and cutting wood (EIA, 2019). However, it was not until the early 20th century that a foundation for wind energy science was developed and specifically applied to converting the mechanical power into electricity via a generator (Veers et al., 2019). Since the 1980s, wind power capacity has increased dramatically worldwide, primarily due to advances in technology and tax and investment incentives offered by governments for renewable energy sectors (EIA, 2019).

Wind turbines (WTs) are developed to harness the wind power to generate electricity. They have become more powerful, more efficient and more affordable (Martino, 2014). Today, wind farms (WFs), which consist of many individual WTs, can generate large quantities of electricity worldwide. The share of US electricity generation from wind was less than 1% in 1990 and nearly 7% in 2018 (EIA, 2019). The wind power generated in the European Union (EU) in 2017 was enough to supply 11.6% of the EU's electricity consumption (WindEurope, 2017). China is investing heavily in wind energy and now has the world's largest wind electricity generation capacity. In 2018, the country installed 20.2 gigawatts (GW) of onshore wind energy, representing 44% of global market share (GWEC, 2019). It is projected that wind energy will supply 30% of all global electricity production by 2050 (BNEF, 2019). To meet this goal, WFs would have to occupy continental-scale areas with a huge number of turbines because of low wind power output per unit area (Wang and Prinn, 2010; Fiedler and Bukovsky, 2011). Given the current installed capacity and the projected installation across the world, WFs are likely becoming a major driver of unprecedented manmade land use change on the Earth.

Wind power is a renewable, abundant, inexhaustible, and affordable energy source, ultimately driven by the Sun (Moomaw et al., 2011; Veers et al., 2019). It is considered to be clean, sustainable and environmentally friendly as it produces no GHG emissions during its operation, emits no toxic substances, waste and air pollution, and consumes no water (UCS, 2013). Despite these benefits, the rapid development of wind power has raised concerns about potential adverse impacts.

Wind is one key atmospheric variable that makes up both the weather and climate of a particular region. Wind power depends on, and in return, will affect the wind. While converting wind's kinetic energy into electricity by turning the propeller-like blades of a turbine around a rotor, WTs reduce the wind speed, change the wind shear, and modify the vertical profiles and surface-atmosphere exchanges of energy, momentum, mass, moisture, and trace gases via increasing surface roughness, changing boundary layer stability, and enhancing turbulence in the rotor wakes. These WT-induced changes could modify the weather and climate at local, regional to global scales and the resulting changes in microclimate conditions over WFs and their wake areas may also influence vegetation activity and crop yields (see more discussion in next section). Hence, understanding WT-atmosphere-surface interactions and assessing potential WF-induced environmental impacts are of significant scientific, societal and economic importance.

Assessing environmental impacts of wind energy is a relatively new field. In recent years, there has been an increasing number of studies addressing WF impacts on meteorology, particularly using weather and climate models. Even though debates exist regarding the regional to global-scale effects, modeling studies, mostly based on simple parameterizations and hypothetical WFs, agree that WFs can significantly affect local-scale meteorology. However, it is well known that these models have large uncertainties in simulating local to regional weather and climate and in describing the complex WT-atmosphere-surface interactions.

Unfortunately, WFs are often commercial properties and observed information on meteorological variables in and around WFs is not publicly available. There are only a few field campaigns over operating WFs and the measurements are often for very short periods and from limited sites. Therefore, more observational evidence of WF effects over longer periods and at larger spatial scales is needed. Recently, more ground observations, remote sensed data and reanalysis products have been used to detect, quantify and attribute the WF impacts on ABL structure, near-surface meteorology, and convective mechanisms. In particular, the use of remote sensing data is of increasing importance for assessing WF impacts with spatial detail.

In this chapter, we will review our current understanding of the impacts of onshore WFs on weather, climate, and vegetation. As previous studies on this topic have been largely carried out by numerical simulations and only a few of them were validated against observations, here we will include more recent progress using observations in this review.

2 Wind turbine-atmosphere-surface interactions

2.1 Wind turbine wake effects

WTs are placed in the ABL that is the lowest layer of the atmosphere. Because of its location, the ABL is tightly connected with the land surface. The WF impacts result from the nonlinear synergistic/competitive interactions between several processes in the ABL that go on to affect the surface. On one hand, WTs extract momentum from the air flow and thus reduce the wind speed behind the turbines (Frandsen, 1992; Vermeer et al., 2003; Wisser et al., 2011). Since turbulence intensity is a function of wind speed (Stull, 1988), lower wind speeds likely reduce turbulent mixing. On the other hand, two different mechanisms increase turbulence in the wake. The first mechanism is the spinning of turbine rotors that increases turbulence at different length scales. The second mechanism is driven by the momentum deficit in the wake where the wind shear triggers small turbulent eddies that attempt to

reduce the deficit primarily by transporting momentum downwards from high wind speed regions above the WT. Both of these processes lead to enhanced wake turbulence causing an increase in the vertical turbulent mixing and surface fluxes (Frandsen, 1992; Petersen et al., 1998; Vermeer et al., 2003; Baidya Roy and Traiteur, 2010). A modeling study by Calaf et al. (2011) found that under neutral stability conditions, the latter effect is stronger than the former, leading to a net increase in the turbulence and surface fluxes within WFs. Simply put, the spinning rotors of WTs generate turbulence in their wakes—just like the wake from a boat in water. Due to the turbulent nature of the wakes, vertical mixing of lower and upper level air also increases in regions downwind of WFs, and the wakes can spread a long distance downwind of the WTs and induce atmospheric changes over a range of scales (Barthelmie et al., 2004; Rhodes and Lundquist, 2013; Rajewski et al., 2013).

2.2 How wind turbines modify atmosphere-surface interactions

The surface-atmosphere exchanges of energy, momentum, mass, moisture, and trace gases are the fundamental physical processes that determine land-atmosphere interactions. The presence of WTs in the ABL could redistribute local temperature, humidity, and surface sensible and latent heat fluxes and thus modify significantly the surface-atmosphere exchanges (e.g., Calaf et al., 2011; Lu and Porté-Agel, 2011; Zhang et al., 2013; Pryor et al., 2018).

The increased vertical mixing changes the vertical ABL temperature profile and near-surface air temperatures (Baidya Roy and Traiteur, 2010) that leads to a change in land-atmosphere temperature gradients and consequently a change in surface heat flux (Baidya Roy, 2011). Based on the available information from theoretical and modeling studies we can construct plausible scenarios on how WTs may affect near-surface meteorological variables within WFs. Surface sensible heat flux is primarily determined by land-atmosphere temperature gradient and buoyancy (Stull, 1988). Turbulent transport of heat in the WT wakes can affect the gradient and buoyant production/consumption terms, thereby affecting surface layer air temperature and land surface temperature (LST).

Consider a stably stratified ABL with little to no buoyant convective transport. In this environment warm air overlies cooler air and it typically occurs when the ABL is in contact with a cold surface such as radiatively cooled dry land at night. If the turbulence in the turbine wakes is stronger than the background turbulence, vertical mixing will be enhanced. Increased vertical mixing will mix warm air down and cool air up, leading to a warming of near-surface air. This warming will decrease the land-atmosphere temperature gradient (more negative) and increase the downward heat flux from the atmosphere to the surface. Consequently, the near surface air temperature and LST are likely to increase.

Alternatively, if ABL is unstable with strong convection, such as that at daytime, enhanced mixing due to wake turbulence will lead to a cooling of near-surface air and LST. However, this cooling will also reduce buoyant convection. Additionally, wake turbulence will reduce the amount of energy available for convection. Since convection results in upward heat transport, the reduction in convection will lead to a heat build-up near the surface. Hence, the net effect of WFs on near-surface air temperatures, land-atmosphere heat exchanges and LST will result from a competitive interaction between the gradient and buoyancy forcing.

If the ABL is very well-mixed and exhibits a neutral stability profile with near-zero vertical temperature gradient in the atmosphere, enhanced mixing due to WTs will not change the land-atmosphere temperature gradient, surface layer temperature and LST. However, in some cases WTs may still reduce the intensity of convection and increase surface layer air temperatures. Consequently, the surface sensible heat flux may decrease leading to an increase in LST.

Enhanced vertical turbulent mixing due to WTs can also have a strong effect on humidity in the ABL and latent heat flux from the surface. Just like temperature, the effect on humidity is directly correlated with the vertical profile. The major source of water vapor in the ABL is evapotranspiration (ET) from the surface. Hence, in most cases, the water vapor content of the ABL decreases with height. Enhanced turbulent mixing transports moist air up and dry air down thereby redistributing moisture more uniformly throughout the lower ABL. This reduces the water vapor content of the lower ABL. As the air becomes drier, ET from the surface, which is primarily driven by surface-atmosphere moisture gradients, increases. The opposite effect of decrease in ET can occur in cases where the vertical humidity gradient is positive, i.e., the ABL is dry near the surface and moist aloft.

These WT-induced changes are expected to have some local impacts on short-term weather and long-term climate at the immediate vicinity of WFs. Such impacts, if spatially large enough, could modify the weather and climate at regional to global scales depending on the location, magnitude, and extent of wind power deployment. Despite an increasing amount of research effort on this topic, there are still many critical knowledge gaps in our understanding of WT-atmosphere-surface interactions and WF impacts on weather and climate.

2.3 How wind turbines interact with vegetation

Plants respond to the climate where they are growing and plant growth is mainly controlled by microclimate conditions such as sunlight, temperature, humidity, moisture, and wind. Most WFs are built over vegetated surfaces such as grasslands and croplands. For example, the Great Plains, home to the US's wheat and corn production, has the richest onshore wind resources across the nation. The abundance of realized and potential wind resources over this region stimulates discussion on the interactions between WFs and agriculture. While the collocation of WFs with natural vegetation or intensively managed agricultural production is possible, it brings up the concerns of whether the widespread deployment of WFs will affect vegetation activity and crop yields resulting from WF-induced microclimate changes over WFs and their wake areas.

It is interesting to note that commercial farmers have used giant fans or wind machines to increase turbulent mixing, promote plant growth, and protect their crops from frost (Snyder and de Melo-Abreu, 2005; Xia and Zhou, 2017). One important question is whether operating WTs may generate similar effects. The WF-induced microclimate impacts may be mostly local and limited to surface and near-surface ABL, but this is the layer where plants grow. In particular, the impacts of WFs on microclimate are of the order likely to influence plant productivity and carbon cycling. For example, Armstrong et al. (2014) suggested that WFs can significantly change local ground-level microclimate (e.g., soil temperature, carbon cycle and soil moisture) to a magnitude that could affect the fundamental plant-soil processes governing plant's biological growth. Meyers and Meneveau (2012) showed that the wakes of WTs may extend the WF-induced changes in microclimate well beyond the small local turbine "footprint". Prasad et al. (2007) observed that the increase in nighttime temperature would decrease grain production from wheat. Lu et al. (2013) indicated that near-surface warming could stimulate ecosystem photosynthesis as well plant C pools. Moreover, turbine enhanced turbulence could affect local hydrometeorology and potential biogenic gas (CO_2 , CH_4 , and N_2O) concentration profiles in the near-surface ABL (Baidya Roy et al., 2004; Rajewski et al., 2013, 2014). Rajewski et al. (2014) presented some evidence that turbine wakes could enhance daytime moisture and CO_2 fluxes several hundred meters downstream, with enhancement of net upward CO_2 and downward heat fluxes at night. Large-scale WFs are simulated to increase evapotranspiration (ET) under stable atmospheric conditions (Baidya Roy et al., 2004; Keith et al., 2004). Field measurements document that enhanced turbulence promotes ET rate (McNaughton, 1988; Rajewski et al., 2014). Likely, operating WFs may potentially modify soil moisture (SM) content and thus alter SM availability for plant photosynthesis during the growing season. However, we know very little about WT-vegetation interactions and WF impacts on plant and agriculture due to paucity of observations and our limited knowledge of relevant biogeochemical and biogeophysical processes.

Therefore, understanding WT-atmosphere- surface interactions and quantifying and projecting WF impacts on weather, climate and vegetation activity are of crucial importance for sustainability and growth of renewable wind energy as well as agricultural activity.

3 Methods for assessing wind farm impacts

3.1 Observational methods

Ground observations, remote sensed data and reanalysis products could be used to detect, quantify and attribute the WF impacts over various operating WFs under different meteorological and terrain conditions. High temporal, coarse spatial resolution data provide the capability to identify the changes in the diurnal cycle, while high spatial, low temporal resolution data provide spatial details of the changes. Reanalysis and sounding data such as wind, temperature and humidity profiles can help examine ABL structure and stability. In particular, the availability of various high-quality remote sensing products such as from the Moderate Resolution Imaging Spectroradiometer (MODIS) instrument onboard the NASA's Terra and Aqua satellites can provide detailed changes at 250 m to 1 km resolutions. Below we summarize two major types of approaches currently used to assess the WF impacts: (1) time series analysis and (2) spatial pattern analysis. These approaches can be applied to several key meteorological and biological variables (e.g., temperature, wind, precipitation, albedo, soil moisture, land cover/use, vegetation greenness, and surface radiative and nonradiative fluxes), and can be combined with composite analysis.

3.1.1 Time series analysis

Three methods have been used to assess the WF impacts on key variables as a function of time (e.g., Baidya Roy and Traiteur, 2010; Zhou et al., 2012, 2013a,b). The central idea is to compare the differences between two time series (with and without the WF impacts). The time series of detected impacts can be correlated with the number of operating WTs, the amount of power generation, wind speed and other WF-related variables.

The first method is to examine the differences observed between two sites (e.g., Baidya Roy and Traiteur, 2010), one with WF impacts and one without, for ground observations, or between two groups of pixels, WF pixels (WFPs) and nearby-non-WF pixels (NWFPs), for remote sensed images (e.g., Zhou et al., 2012, 2013a,b). Similar methods have been extensively used to estimate urban heat island effects by comparing observed temperatures in urban stations with their nearby rural ones (Gallo and Owen, 1999; Peterson, 2003). It is assumed that the urban and rural stations share the same regional-scale background atmospheric conditions and thus their differences are due primarily to local urban effects. Similarly, the observed differences between two sites or two groups of pixels can be used to quantify the impacts of operating WTs.

The second method is to examine the differences between observed and reanalysis data (observed minus reanalysis) over the WFs (e.g., Zhou et al., 2012, 2013a). Similar methods were developed to estimate the effects of urban heat island and other land use change (Zhou et al., 2004; Wang et al., 2013). The reanalysis is strongly influenced by observational atmospheric variables and little by changes in the land surface, and thus the differences (observed minus reanalysis) are postulated to represent the impacts of land use change (Kalnay and Cai, 2003). This method assumes that the regional-scale background atmospheric conditions are mainly captured by the reanalysis while the local WF impacts are not, and so their differences are due primarily to the WF effects.

The third method is to examine the differences between observed and reconstructed data (observed minus reconstructed) over the WFs (e.g., Zhou et al., 2013b). Statistics and signal processing methods such as empirical orthogonal function (EOF) analysis can be used to decompose the observed 2-dimensional (2D) fields into different spatial patterns of variability (i.e., EOF modes) and their time variations (i.e., EOF time series). EOF analysis is often used to study spatial patterns of climate variability and how they

change with time (Bjornsson and Venegas, 1997). It describes the degree of coherence of spatial variations and gives a measure of the “importance” of each pattern, with the first pattern being responsible for the largest part of the variance, the second for the largest part of the remaining variance, and so on. The first several leading EOF modes represent mainly the large-scale features, not the local WF effects, and so can be used with their corresponding time series to reconstruct the observational data without the WF impacts.

3.1.2 Spatial pattern analysis

Three methods, corresponding to the aforementioned three methods for time series analysis, have been used to quantify the WF impacts in the spatial patterns between two different (pre- and post-WT) periods. The central idea is to compare the spatial differences between these two periods (with and without the WF impacts), resulting from two components, (1) the changes in the regional-scale background atmospheric conditions, which vary naturally even without WFs, plus (2) the WF-induced local changes. Removing the former from the spatial differences is the key to obtain the latter. It is assumed that the WF-induced changes should couple spatially with the layout of WTs. These methods work best for the 2D fields such as reanalysis data and remote sensed images.

The first method is to examine the spatial differences in observations over the WFs between the pre- and post-WT periods. The regional-scale background atmosphere could be obtained by averaging the data over a much large region covering the WFs, and so its changes between these two periods can be simply removed from the spatial differences in the original data (e.g., Zhou et al., 2012, 2013a).

The second method is to examine the spatial differences in observed and reanalysis (observed minus reanalysis) data over the WFs between the pre- and post-WT periods. As stated previously, the changes in the regional-scale background atmosphere are captured by the reanalysis and thus can be easily removed (e.g., Zhou et al., 2012, 2013a).

The third method is to examine the spatial differences between observed and reconstructed data (observed minus reconstructed) over the WFs between the pre- and post-WT periods. As stated previously, the changes in the regional-scale background atmosphere can be captured by the reconstructed data from the first several leading EOF modes and their time series and thus be easily removed (e.g., Zhou et al., 2013b).

3.1.3 Other observational methods

Potential WF impacts are also assessed by other approaches, including statistical analysis such as regression models (Chen, 2019) and econometric analysis such as reduced-form models (Kaffine, 2019). Here we will not detail these approaches due to their limited usage in WF studies.

3.2 Modeling methods

Impacts of WFs on meteorology are often quantified using weather and climate models based on numerical experiments. The experiments often include a control run and a group of sensitivity experiments, i.e., model simulations with and without the presence of WFs, and the differences between the control run and the sensitivity experiments are used to assess the WF impacts.

Weather and climate models are computer programs that solve the set of equations describing the processes that govern the earth’s weather and climate systems. The equations range from the simple ideal gas law that describes the relationship between temperature, pressure and density, to the complex Navier-Stokes’ equations that is a system of partial differential equations describing how airflow is affected by various forces like pressure gradient, gravity and friction. The models solve conservation equations for mass, momentum, heat and various moisture species using parameterizations for turbulent mixing, radiation, microphysics and surface fluxes. Overall, the set of equations is too complex that there are no known exact solutions to them. That is why, we use advanced numerical methods to find approximate solutions. Studies show that if the underlying physics of various atmospheric processes are well understood and the equations representing the processes are robust, then the approximate solutions are pretty close to reality. Therefore, it is crucial to first understand how WTs and WFs interact with the airflow and then develop equations for these interactions to be represented in weather and climate models.

It should be noted that weather and climate models are typically run at spatial resolutions of 1–100 km. Clearly, such resolutions are so coarse that individual WTs and often the entire WFs are smaller than one grid cell of the model. Hence, WTs and WFs are approximated as sub-grid parameterizations. There are fundamentally two major different ways in which WTs have been parameterized in numerical models: (1) the enhanced roughness length, and (2) the elevated momentum sink and turbulent kinetic energy (TKE) source. All of them are based on physics but with different levels of complexity.

3.2.1 The enhanced roughness length parameterizations

The simplest method is based on the observations that WFs behave like an obstacle that slows down the wind, and hence WFs are parameterized as obstacles with high roughness length that generates strong frictional drag thereby reducing the wind speed. A major problem in this approach is that we do not have any quantitative estimates of the roughness length or the frictional drag due to a WF. Because of this, Wang and Prinn (2010, 2011) resorted to using different arbitrary values for their numerical experiments in a General Circulation Model (GCM). For example, in one experiment, they assumed the roughness length of a WF similar to that of a deciduous needle-leaf tree, implying that a WF behaves just like a deciduous needle-leaf forest. Keith et al. (2004) and later Kirk-Davidoff and Keith (2008) adopted the same enhanced roughness length approach in their GCM studies but

used a more realistic way to quantify the roughness length. They contended that the drag force should be equal to the power generated by a WF. They started with the WF power output and back calculated the surface drag exerted by a WF from that value. From the surface drag, they estimated the roughness length, assuming neutral stability conditions. This method is intuitive but has a number of conceptual drawbacks. A WF does not behave like a typical obstacle such as a hill or a dense forest. WTs in a WF are spaced far apart, allowing air to flow between them. Moreover, the turbine rotors are not placed on the land or water surface but rather at heights 100 m or more. In spite of these limitations, the surface drag approach is widely used by the climate community perhaps because it is relatively easy to implement in GCMs.

3.2.2 The elevated momentum sink and TKE source parameterizations

The second and more conceptually rigorous approach to represent WFs was developed by Baidya Roy et al. (2004) and later used by Baidya Roy and Traiteur (2010). They observed that a WT absorbs energy from the wind and generates turbulence in its wake. Based on this observation, they approximated a WT as an elevated sink of momentum and a source of TKE. The challenge in this approach was how to quantify WT behavior. They assumed that the power coefficient (C_p) of the turbine is 0.4, i.e., it absorbs 40% of the energy that passes through the rotor to generate power. Also, using data from an operational WF, they assumed that the turbines generate $5 \text{ m}^2/\text{s}^2$ (approximately 6 J) of TKE in the wake.

Subsequent studies have made two major improvements to this “elevated momentum sink and TKE source” approach. The assumption of a constant C_p is not realistic because C_p is a function of the turbine type and varies with wind speed. Taking this fact into account, Baidya Roy (2011) improved the parameterization of Baidya Roy et al. (2004) by using wind-speed dependent C_p values obtained from the power curve data of a commercial turbine. The turbulence generated in wake was still constant with wind speed.

The second improvement in the approach was to incorporate realistic estimates of TKE generated by turbines. Fitch et al. (2012) and Adams and Keith (2013) solved this problem by using data from commercial WTs. The energetics of a WT can be explained by two parameters: the thrust coefficient (C_t) that gives the fraction of energy removed from the wind flow by the turbine, and the power coefficient C_p that gives the fraction of energy in the flow that is converted to electricity. Fig. 1 shows the typical patterns of C_t and C_p of a commercial WT. They assumed that the part of the energy removed from the wind that is not converted to electricity ($C_t - C_p$) is converted to turbulence in the wake. This is a reasonable assumption because other losses such as frictional dissipation by the turbine structure are likely to be small. This assumption allowed them to quantify the TKE added in a robust and realistic manner. The effect of the added sophistication in quantifying the momentum sink and the TKE source is evident in Fig. 2.

Within this broad paradigm of the “elevated momentum sink and TKE source” approach, several studies have proposed and implemented alternative methods to quantify the turbulence. For example, Jacobson and Archer (2012) and Marvel et al. (2013) assumed that wake turbulence can be completely ignored. Blahak et al. (2010) have added a correction term to the momentum sink to account for mechanical and electrical losses with the added TKE being proportional to the extracted kinetic energy. Abkar and Porté-Agel (2015) used an analytical approach to approximate the added TKE as a function of the upstream velocity and the thrust coefficient. Their parameterization can take into account the effects of WT density, WF layout and wind direction using a correction parameter, the value of which was estimated from a Large-Eddy Simulation (LES) model simulation. Along similar lines, Pan and Archer (2018) have used LES results to empirically derive the momentum sink and TKE source terms. However, the parameterizations of Abkar and Porté-Agel (2015) and Pan and Archer (2018) are yet to be implemented in weather and climate models. It may be almost impossible to do so because that would require numerous LES simulations for all possible wind directions and WF layouts.

Volker et al. (2015) developed a new method to estimate the increased turbulence in the wakes of WTs. They contended that wake turbulence was mechanically generated due to increase in wind shear as the wake expands in space. In their parameterization,

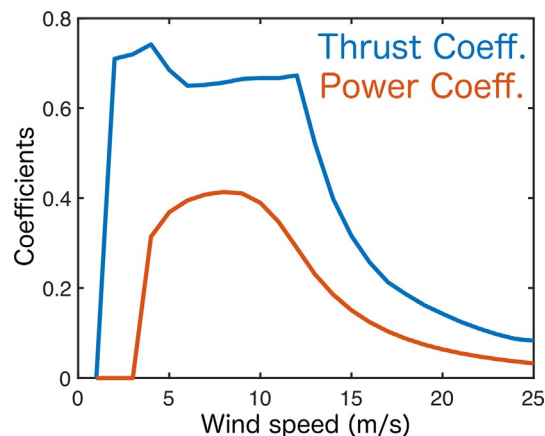


Fig. 1 Thrust (C_t) and power (C_p) coefficients of a Gamesa G80–2.0 MW wind turbine. The data for the Gamesa turbine was accessed on September 7, 2010, available online at <http://www.gamesacorp.com/files/File/G80-ingles.pdf>.

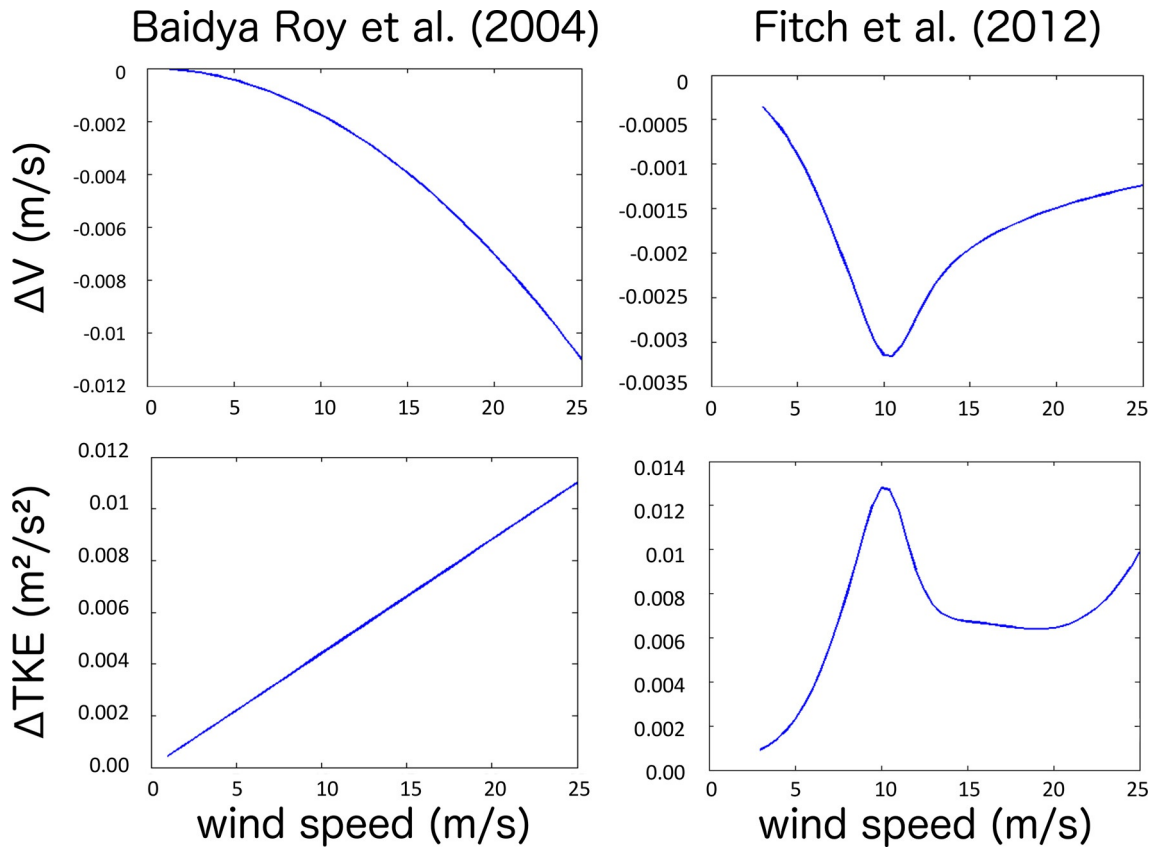


Fig. 2 The difference between the early Baidya Roy et al. (2004) and recent Fitch et al. (2012) wind turbine parameterization schemes in terms of wind speed (top) and TKE in the wake (bottom).

they first developed equations to approximate the spatial expansion of a WT wake and enhanced turbulent transport in the atmosphere due to the increase in shear. They implemented this parameterization in the WRF model and showed that this method generated less TKE compared with Fitch et al. (2013). However, due to lack of appropriate field observations on the spatial structure of WT wakes, the parameterization developed in this study is yet to be rigorously evaluated.

Recently, Redfern et al. (2019) have proposed an improved version of the Fitch et al. (2012) scheme in WRF. Instead of using the hub height wind speed to calculate the momentum sink and TKE source terms, they used “rotor equivalent wind speed” that accounted for magnitude and directional shear in the wind across the rotor disk. They found that this modification had marginal impacts except for cases having highly nonlinear wind shear with wind speeds near the turbine cut-in or cut-out speeds.

Due to its realistic representation of WT behavior, the “elevated momentum sink and TKE source” parameterization has become the tool of choice for mesoscale modelers interested in investigating the WF effects on meteorology. Numerical simulations with this parameterization have been shown to match well with observations of ABL meteorology and power generation (Baidya Roy and Traiteur, 2010; Lee and Lundquist, 2017). In comparison, the “enhanced roughness length” parameterization performs poorly as it does not allow wind to flow below or around the rotors the way it occurs in nature. Fitch et al. (2013) showed that the roughness length parameterization significantly overestimated the impacts on temperature and surface fluxes and at times got the sign of the changes wrong, concluding that “the enhanced surface roughness approach is not an appropriate option to represent WFs or explore their impacts.” Thus, mesoscale models provide an opportunity to investigate the flow in and around large WFs as a whole, and to assess the resulting impact on local and regional meteorological conditions. One widely used mesoscale weather forecast model for WF impact studies is the Weather Research and Forecasting (WRF) model (Skamarock et al., 2008; Skamarock and Klemp, 2008). The WRF has been developed to simulate mesoscale weather phenomena in a wide range of scales, from large scale synoptic systems that extend over areas of several hundreds of kilometers to phenomena that occur at scales of tens of kilometers.

3.2.3 Other modeling methods

It is important to note that the above discussion is confined to weather and climate models that are used to explore the environmental impacts of WFs, in which WTs and WFs are approximated as sub-grid parameterizations due to coarse model resolutions. There are other types of models such as LES and Computational Fluid dynamics (CFD) models that have been used to study aspects of WT behavior at very high resolutions. For example, LES models have spatial resolutions of 1–10 m while CFD models are run at resolutions that are several orders of magnitude finer. Because of the high resolution, these models do not need

sub-grid parameterizations to represent WTs. LES models can resolve WT wakes (Churchfield et al., 2012; Vanderwende et al., 2016) while CFD models can even resolve WT blades (Cai et al., 2016). They also use prognostic equations for second order moments representing turbulent transport instead of using TKE-based diagnostic approximations. These high-resolution models are able to resolve detailed fluid dynamics and the complex interactions between individual WTs and their airflow. However, their applications for weather and climate studies are limited because they are too computationally expensive to simulate large WF impacts and can be used only under idealized conditions (Fitch et al., 2012, 2013).

4 Weather and climatic impacts of onshore wind farms

In this section, the WF impacts on weather and climate discussed are roughly divided into two major spatial scales: (1) local to regional and (2) large to global. The former includes observational and mesoscale modeling studies for WFs at county and state/province levels, while the latter consists of modeling studies for WFs at country and continental levels.

4.1 Local to regional impacts

Previous research work has assessed local to regional impacts of WFs on weather and climate. Physical reduction in downwind wind speed and temperature changes in the vicinity of WFs are found in both observational and modeling studies. Possible impacts on land surface properties, precipitation and wind patterns are identified using simulations or observations.

4.1.1 Impacts on land surface properties

The land surface functions as the lower boundary conditions of the atmosphere for the weather and climate system. The large deployment of WTs may have some impacts on land cover/use and land surface properties associated with the turbine “footprint” (i.e., turbine blades, towers, access roads, etc.) within the WFs. However, the “footprint” area occupies only a small percentage, typically ranging from 2% to 5%, of the total land area of WFs because substantial inter-turbine spacing is required to maximize turbine efficiency in capturing wind and also to avoid turbine wake effects (Wiser et al., 2011). This allows agriculture, ranching and certain other activities to continue within the WF area.

Zhou et al. (2012) used MODIS data (e.g., land cover, albedo, and vegetation) to detect changes in land cover/use and land surface properties over four large WFs over West-Central Texas, United States. They found small and insignificant changes in land cover, surface albedo, and vegetation cover over the WFs, possibly related to the turbine “footprint,” which, however, are too small to explain the detected WF impacts such as warming seen by MODIS. Shen et al. (2017) mapped the damage of grasslands for a 10 million-kilowatt wind power base in Jiuquan City, Gansu Province, China, using both satellite images and measured field data. They showed that WF construction did cause vegetation damage and other ecological problems, but this damage accounted for only ~2.2% of the studied WF areas (see more in Section 5.1).

4.1.2 Impacts on temperatures

Turbulence in the wakes of WTs increases the vertical heat transfer in the ABL thereby modifying the vertical temperature profile in the ABL, land-atmosphere heat exchange and land surface temperature (LST). There are many observational and modeling studies on this topic.

There are a few short-term observational studies at or near WFs. Baidya Roy and Traiteur (2010) first used in situ observations for 1.5 months from a WF in California to explore the relationship between ABL stability and changes in near-surface air temperature. They found that there was a net downward transport of warm air causing an increase in surface temperature in a stably stratified boundary layer environment. In the daytime when the lapse rate was negative, a net downward transport of cooler air caused a surface cooling effect. Smith et al. (2013) conducted a field campaign in a large WF in the Midwestern US for 47 days and identified a strong surface warming of 1.9 °C in the wake of the WF at night but no substantial warming or cooling signals during the day. Rajewski et al. (2013) measured air temperature, surface fluxes and other variables in a 200-turbine WF in central Iowa as part of the Crop Wind Energy Experiment (CWEX) campaign. They observed a small cooling (<0.75 °C) in 9 m air temperatures downwind of the WF during the day and a strong warming (up to 1.5 °C) at night.

In contrast to local point measurements from field campaigns, satellite remote sensing provides a unique and new way to detect and quantify WF impacts with spatial details over large areas. Zhou et al. (2012) presented the first observational evidence for large WFs on LST in West-Central Texas using MODIS LST data at 1 km resolution for the period 2003–2011. Note that the majority of WTs were built during 2005–2008. They found a significant areal mean warming trend of up to 0.72 °C per decade at night but no noticeable effects during daytime. This warming was attributed primarily to WFs because: (1) the spatial pattern of the warming coupled very well with the geographic distribution of WTs (Fig. 3), and (2) the year-to-year LST over the WFs shows a persistent upward trend from 2003 to 2011, consistent with the increasing number of operating WTs with time (Fig. 4).

Fig. 3 shows the spatial pattern of MODIS summer nighttime LST differences between two (post-turbine minus pre-turbine) periods. The left panel is the LST differences (2011–2009 average minus 2003–2005 average), in which the background LST interannual variability was removed. The right panel is the LST differences between two individual years (2010 average minus 2003 average). Note that the background LST in 2010 and 2003 is similar, and so the LST differences (2010 minus 2003) primarily reflect

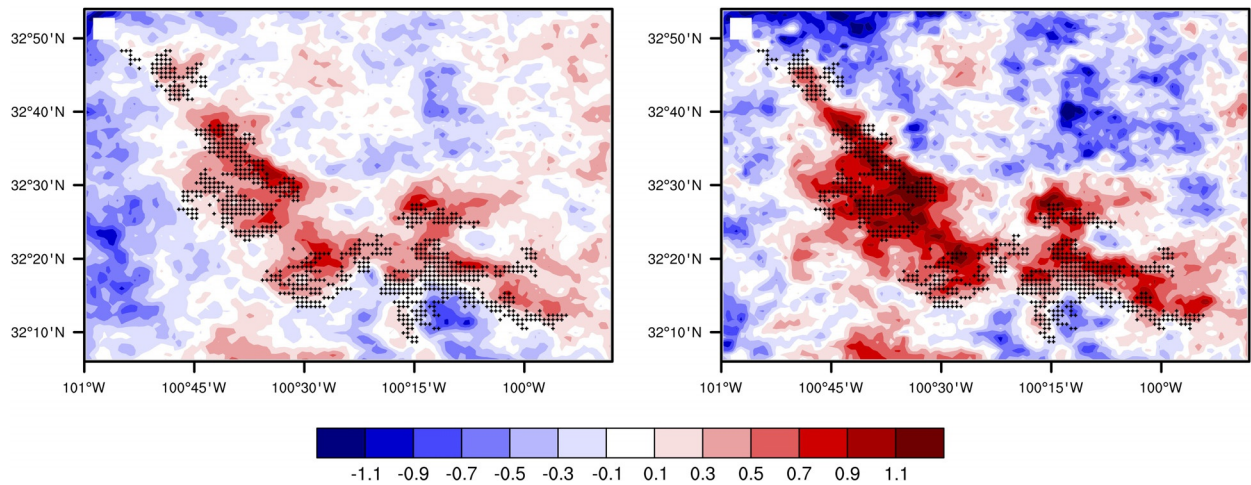


Fig. 3 MODIS June-August nighttime LST differences ($^{\circ}\text{C}$) (post-turbine period minus pre-turbine period) for the period of 2003–2011: (left panel) 2011–2009 average minus 2003–2005 average. (right panel) 2010 minus 2003. Black dots represent individual WTs. Reproduced with permission from Fig. 2A and B in Zhou L, Tian, Y, Baidya Roy S, Thorncroft C, Bosart LF and Hu Y (2012) Impacts of wind farms on land surface temperature. *Nature Climate Change* 2: 539–543.

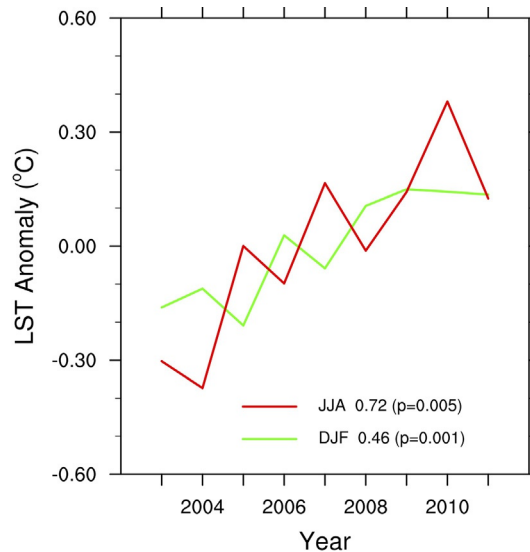


Fig. 4 Time series of MODIS nighttime LST differences (WFPs minus NWFPs) in June-August (JJA) and December-February (DJF) for the period 2003–2011. Linear trends ($^{\circ}\text{C}/10$ years) and their significance levels (p values) estimated using least squares fitting are shown. Reproduced with permission from Fig. 3B in Zhou L, Tian, Y, Baidya Roy S, Thorncroft C, Bosart LF and Hu Y (2012) Impacts of wind farms on land surface temperature. *Nature Climate Change* 2: 539–543.

the LST change due to the operating WTs. Evidently, the WF-induced warming couples very well with the geographic distribution of WTs in both panels.

Fig. 4 shows the interannual variations of MODIS nighttime LST differences (WFPs minus NWFPs) in summer (June–August) and winter (December–February) for the period 2003–2011. Evidently, there is a persistent warming trend from 2003 to 2011, consistent with the increasing number of operating WTs with time. The linear trends, $0.72^{\circ}\text{C}/10$ years. in summer and $0.46^{\circ}\text{C}/10$ years. in winter are both statistically significant at $P < .01$ level.

Later, Walsh-Thomas et al. (2012) used satellite images from Landsat 5 Thematic Mapper to study temperature changes over the San Gorgonio Pass WF from 1984 to 2011 and found a consistent warming trend observed downwind of the WF. Zhou et al. (2013a) examined the seasonal and diurnal variations of the WF-induced warming effect in West-Central Texas under different data quality controls of MODIS data. Their results consistently showed a nighttime warming signal of 0.31 – 0.70°C across all seasons, with the largest warming in summer, while daytime results were inconclusive. Zhou et al. (2013b) ruled out the possibility that the warming signal could be an artifact of varied surface topography or land use/cover change in and around the WF region.

Harris et al. (2014) and Slawsky et al. (2015) furthered Zhou's work by examining the impacts of five WFs in Iowa and three WFs in Illinois using MODIS LSTs for the period 2003–2013, respectively. Similar results are found for the eight WFs in both states:

consistent warming signal was detected at nighttime LST but there was no apparent impact on daytime LST. An areal mean WF-induced warming in LST was estimated to be 0.18–0.39 °C in Illinois and 0.12–0.44 °C in Iowa. This provides further observational evidence that WFs can cause surface warming at nighttime. However, the warming signals vary seasonally (i.e., the strongest LST warming were observed in winter in Illinois). Using data from nearby soundings and surface observations, Slawsky et al. (2015) showed that stronger winds in winter corresponded to a stronger nighttime warming signal, while a strong, shallow temperature inversion in summer corresponded to a more pronounced spatially coupled nighttime warming signal with the WT layout.

Xia et al. (2016) examined the effects of TKE and static stability on the seasonal and diurnal variations of WF-induced LST over the same WFs studied by Zhou et al. (2012). Using SoDAR and 3D sonic flux data from the *Wind Forecast Improvement Project (WFIP)* (Freedman et al. 2014) and high-resolution upper air sounding data, they showed that variations in the ratio of TKE induced by WTs relative to the background TKE helped to explain not only the day-night contrast of the WF impact on LST, but also most of the seasonal variability in the turbine-induced nighttime LST changes. In addition, atmospheric stability also mattered in determining the sign and strength of the net downward heat transport as well as the magnitude of the background TKE.

Other observational studies (Walsh-Thomas et al., 2012; Smith et al., 2013; Armstrong et al., 2016; Chang et al., 2016; Rajewski et al., 2016) also confirmed similar WF impacts on surface/near-surface temperature. The only exception is Moravec et al. (2018), who examined 5 months of measurements from automatic stations for a 21-WT WF located on the Ore Mountain in Czech Republic, and found no clear evidence of spatially and temporally stable impact of the WF on near-surface temperature.

In the regional modeling domain, Baidya Roy et al. (2004) first parameterized the effect of WFs into a mesoscale model and showed that WFs can induce daytime cooling and nighttime warming due to heat flux transport caused by the rotator blade. Their subsequent modeling studies (Baidya Roy and Traiteur, 2010; Baidya Roy, 2011) further confirmed that WFs, through their interactions with the ABL, can significantly affect near-surface air temperature and humidity as well as surface sensible and latent heat fluxes. Fitch et al. (2012, 2013) implemented the effect of WT into the community WRF model and examined the mesoscale influences of the hypothetical WF in a diurnal cycle. The simulated WFs produced a warming effect at surface during nighttime while the daytime temperature change was negligible.

Validation of the simulated impacts of realistic WFs has been performed only in three recent papers. Cervarich et al. (2013) first tried to evaluate the ability of WRF model in simulating seasonal variations in LST over real-world WFs in West-Central Texas for the summer in 2010 under realistic boundary conditions. They confirmed the major observational findings of Zhou et al. (2012) but their simulated LST warming signals were too weak and did not show strong spatial correspondence to the layout of the WTs. After refining the simulations of Cervarich et al. (2013), Xia et al. (2017) confirmed that the WRF model was moderately successful at reproducing the observed spatiotemporal variations of the background LST in West-Central Texas. Fig. 5 shows the simulated LST differences with and without the presence of WTs for July 2010–2014. Clearly, the WF-induced warming signal and the WT layout are well spatially coupled. However, there was a distinct downwind cooling effect extending as far as 40 km away from the WFs, which has not been confirmed by previous field campaigns and satellite observations. Two physical mechanisms, turbulent heat flux divergence and 3D temperature advection, were confirmed to be mainly responsible for the simulated WF impacts on temperature (Xia et al., 2019).

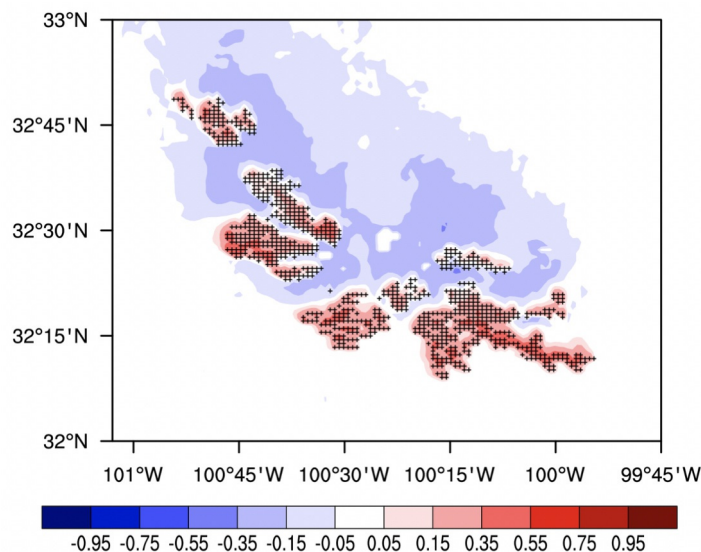


Fig. 5 July nighttime LST (°C) differences between simulations with and without the wind turbine parameterization for the post-turbine period (2010–2014). The black dots indicate WFPs and the simulated nighttime LST is averaged from hourly model output between 2200 and 0200 local time. Reproduced with permission from Fig. 8A in Xia G, Cervarich M, Baidya Roy S, Zhou L, Minder J, Freedman JM and Jiménez PA (2017) Simulating impacts of real-world wind farms on land surface temperature using WRF model: Validation with MODIS observations. *Monthly Weather Review* 145: 4813–4836.

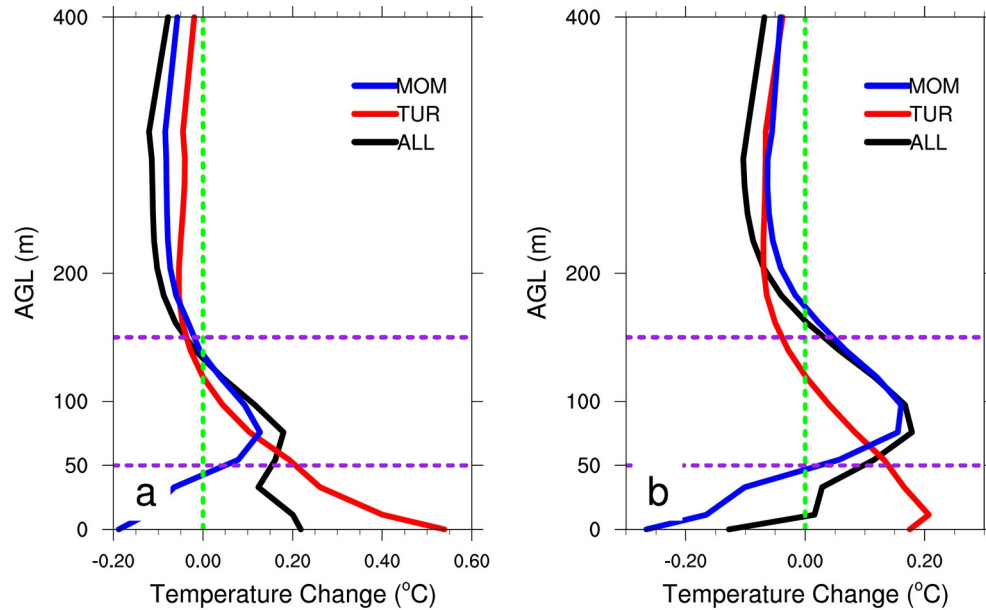


Fig. 6 Areal mean vertical profiles of the simulated WF-induced temperature changes between 19:00 and 06:00 local time from the ALL, TUR and MOM experiments averaged over the WFR and NWFR. The purple lines indicate the rotor disk region. Reproduced with permission from Fig. 4 in Xia G, Zhou L, Minder JR, Fovell RG and Jimenez PA (2019) Simulating impacts of real-world wind farms on land surface temperature using the WRF model: Physical mechanisms. *Climate Dynamics* 53: 1723–1739.

Fig. 6 shows the regional mean vertical profile of WF-induced temperature changes over the wind farm region (WFR) and nonwind farm region (NWFR) at nighttime. The red line (TUR) indicates the temperature profile induced from the TKE effect of the WF parameterization whereas the blue line (MOM) is that from the momentum sink effect of the WF parameterization. The black line (ALL) shows the combined net effects from both the TKE and momentum sink effects. In both WFR and NWFR, the TKE component of the WF parameterizations contributes to the surface warming whereas the momentum sink component contributes to the surface cooling. Owing to their differences in sign and magnitude, the net effect shows a surface warming signal over the WFR but a surface cooling signal over the NWFR. Around the hub-height level, both components contribute to the warming signal. Above the maximum rotor height (150 m), both components contribute to the cooling signal.

To further understand the vertical structure of the simulated temperature changes, Fig. 7 shows vertical cross sections of the simulated temperature changes at nighttime from the ALL experiment. The two green lines at bottom of each figure indicate the location of WFR. Starting from 21:00 local time (LT), the surface warming signal occurs over the WFR while a cooling signal develops above the hub-height level and at the downwind edge of the WFR. At 22:00 LT, the surface warming and cooling signals strengthen. In addition, a secondary warming pattern develops around the hub-height levels and then connects with the surface. From 23:00 LT to 03:00 LT, most of the WF-induced changes, such as the surface warming/cooling signals, the secondary warming signal as well as the cooling above the hub-height level, extend and intensify both horizontally and vertically away from the WFR. From 04:00 LT to 06:00 LT, the simulated temperature changes start to weaken and disappear around 09:00 LT (figures not shown). To the best of our knowledge, most of these detailed changes have not been reported or confirmed in any previous field campaigns or satellite observations.

4.1.3 Impacts on precipitation

The WT-induced changes in the heat and moisture exchange in the interface between surface and ABL may modify the atmospheric stability, vertical moisture transport and large-scale convergence thereby impacting precipitation patterns. However, there are only a few modeling papers but no observational studies on this topic.

Fiedler and Bukovsky (2011) conducted regional climate simulations using the WRF model to study the WF effect on warm-season precipitation in the eastern US. A giant “artificial” WF was represented within the modeling domain, covering 187,000 km² from Texas panhandle to northern Nebraska in the central US and the WF effect was parameterized as drag force acting over the rotor area on the mean wind flow. The results indicated that the presence of a mid-west WF, either giant or small, can have an enormous impact on the weather and the amount of precipitation for one season, consistent with the known sensitivity of long-term weather forecasts to initial conditions. However, the presence of a giant WF had only a slight impact on climate. In the average precipitation of 62 warm seasons, there was a statistically significant 1.0% enhancement of precipitation in a multi-state area surrounding and to the south-west of the WF, possibly due to that the WF somewhat retarded the advection of drier air from the northwest.

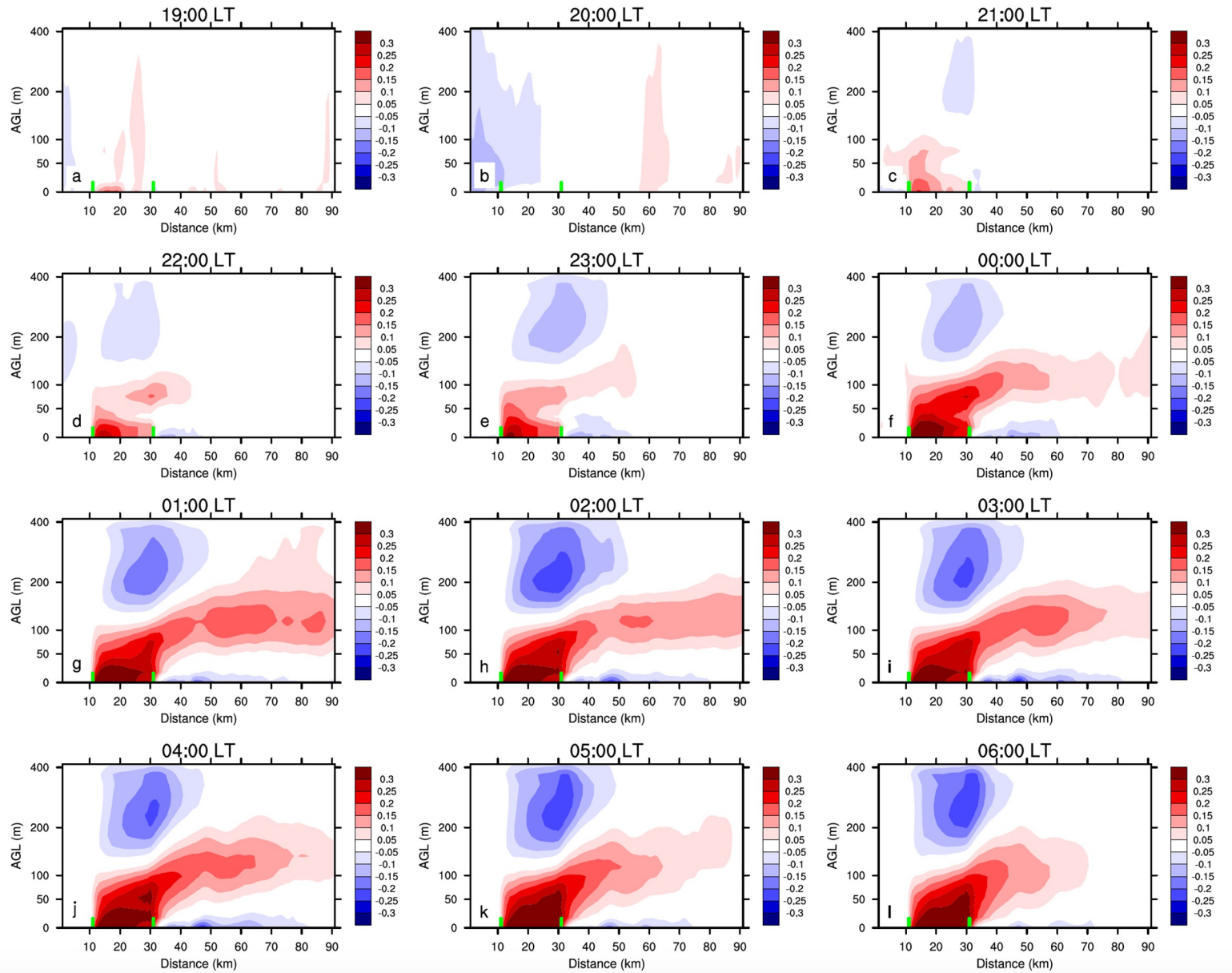


Fig. 7 Vertical cross sections of the simulated temperature differences ($^{\circ}\text{C}$) between simulations with and without the wind turbine parameterization from 19:00 to 06:00 local time (LT). The WF region is located between the two green lines (10–30 km) at the bottom of each figure. Reproduced with permission from Fig. 5 in Xia G, Zhou L, Minder JR, Fovell RG and Jimenez PA (2019) Simulating impacts of real-world wind farms on land surface temperature using the WRF model: Physical mechanisms. *Climate Dynamics* 53: 1723–1739.

Pryor et al. (2018) studied the effects of real-world WFs in Iowa on local and mesoscale climate at convection permitting resolution (4 km) with the WRF model using the Fitch WT parameterization (Fitch et al., 2013). Their results showed that WFs modified wind speeds and near-surface air temperature over grid cells with WTs, and the impacts at larger scales on temperature, specific humidity, precipitation, and sensible and latent heat fluxes were insignificant in any season other than summer. The range of impact was large and spatially incoherent at local scale, while the domain average precipitation signal was very small: a small decrease in precipitation probability and a decrease in season total precipitation of 7 mm (2.6%), most of it being associated with large precipitation events.

Jawaheer et al. (2019) used the WRF model to study the local weather effect of a WF situated at Roches Noires, Mauritius, that has been operational since January 2016. This WF comprises of 11 WTs, each of capacity 850 kW, with an estimated energy production of 81.9 GWh per year. The WRF results were first validated with meteorological data from several local weather stations and then simulations were carried out for the years 2015, 2016 and 2017. The results demonstrated a slight decrease in precipitation, 1 year after installation of the WF.

Other regional modeling studies (Miller and Keith, 2018; Pryor et al., 2020) indicated impacts of very large WFs on precipitation (see more in Section 4.2).

4.1.4 Impacts on wind patterns

The presence of WTs modifies the 3D inflow conditions in the rotor-swept area, the wind shear and turbulence in and downwind of WTs, and thus is expected to modify local to regional wind patterns. Next, we will discuss the impacts of WFs on wind patterns and low-level jets (LLJs).

Previous observations show reduced horizontal wind speed and increased turbulence in the turbine wake region (e.g., Baker and Walker 1984; Christiansen and Hasager, 2005; Rhodes and Lundquist, 2013). For example, Christiansen and Hasager (2005) first used satellite synthetic aperture radar (SAR) to observe the wakes from the Horns Rev and Nysted offshore WFs in Denmark. Within 1–2 km downstream of the WFs, an average wind speed deficit of 8–9% was found, corresponding to an absolute reduction of 0.5–1.5 m/s. The wake recovery depended on not only the ambient wind speed, but also atmospheric stability and the number of turbines in operation. In unstable cases, the wind speed recovered to within 2% of the upstream velocity over a distance of 5 km. For neutral cases, however, at least a 2% deficit persisted over the distance investigated (21 km). Turbulence intensity was increased downwind of the WFs in around a third of the cases studied. Rhodes and Lundquist (2013) collected light detection and ranging (lidar) wind-profile observations during summer 2011 in an operating WF in central Iowa at 20-m vertical intervals from 40 to 220 m above the surface. Measurable reductions in wake wind-speeds occurred at heights spanning the wind turbine rotor (43–117 m), and turbulent quantities increased in the wake. The wind-speed deficit in the wake was largest at hub height or just above, and the maximum deficit occurred when wind speeds were below the rated speed for the turbine. Similarly, the maximum enhancement of TKE and turbulence intensity occurred at hub height.

Model simulations showed WF-induced changes in wind patterns (Barthelmie et al., 2004; Fitch et al., 2012, 2013; Rhodes and Lundquist, 2013; Rajewski et al., 2013; Pryor et al., 2018; Lauridsen and Ancell, 2018; Lundquist et al., 2019; Jawaheer et al., 2019). For example, Lauridsen and Ancell (2018) studied the possible effect of a large hypothetical WF in the central US on tropical and mid-latitude cyclones using WRF simulations. They concluded that large WFs in the Central US can significantly affect midlatitude cyclones, but not tropical cyclones. WFs located close to or upstream of the location of cyclogenesis tended to intensify the cyclone whereas WFs downstream tended to decrease the strength of the cyclone. The effect can be significantly large up to hundreds of kilometers away, including perturbations to the minimum cyclone pressure of 1 hPa and maximum 2 m wind speed of 4 m/s. Based on WRF simulations using a WT parameterization to represent the effects of turbines as elevated drag elements, Lundquist et al. (2019) showed that in stably stratified atmospheric conditions, the decreases in downwind wind speeds can extend for 50 km or more. Jawaheer et al. (2019) analyzed WRF simulated wind data for two selected locations (one upstream and one downstream that is 12 km away from the WF) around the Roches Noires WF and found a decrease in wind speed after the installation of the WF. Also the occurrence of maximum and minimum wind speed was changed as well.

Due to the increase in wind speed and the close distance to ground, LLJs are of particular relevance to wind energy, and are a significant contributor to wind power production in China (Du et al., 2016) and United States (Freedman et al. 2014). The LLJ generally refers to a fast-moving ribbon of air with maximum wind speed at least larger than 12 m/s occurring within the lowest several hundred meters above the ground in the ABL (Bonner, 1968). It has been observed worldwide and attributed to a variety of formation and evolutionary mechanisms (Liu et al., 2014). One of the most studied LLJ is that of the US Great Plains due to its high frequency of occurrence and strong wind speeds spanning hundreds of kilometers along-track and cross-track (Carroll et al., 2019). The US Great Plains is expecting significant WF growth over the coming decades (Veers et al., 2019). The LLJ commonly occurs under favorable synoptic conditions, particularly under the stably stratified ABL at night over land, and thus is often a nocturnal phenomenon, with wind speeds ramping up around sunset and dying down with the rise of the morning convective boundary layer (Carroll et al., 2019).

Key structural characteristics of the LLJs include the frequency of occurrence, the wind speed maximum and its direction, the wind speed maximum height, and the shape and shear of the LLJ wind-speed profile (Zhang et al., 2019). These characteristics are important factors to consider for wind energy. Three major factors affect the amount of *energy a turbine* can harness from the *wind*: wind speed, air density, and *swept area*. The increasing wind speed within the LLJ at the top of the stable boundary layer constitutes major power resources for WTs due to the increased kinetic energy available within the rotor-swept area. However, the LLJ has large wind shear above and below the wind speed maximum height. The occurrence of LLJ can generate significant shear and turbulence

within the atmospheric layer across the turbine rotor plane that affects life span and efficiency of WTs due to the increased potential for aerodynamic loads (Clifton et al., 2013; Zhang et al., 2019).

The impacts of operating WTs on the LLJ in the rotor-swept area and thus the surface-atmosphere exchanges are expected to be maximized at nighttime as the LLJ height decreases with an increase in atmospheric stability (Zhang et al., 2019). So far, numerical models have been used to describe the interactions of WTs with atmospheric flow, and simulations show the WF impacts the LLJ within the WF area and downwind, mainly at nighttime. For example, Lu and Porté-Agel (2011) integrated a 3D large-eddy simulation with an actuator line technique to examine the characteristics of WT wakes in a hypothetical large WF inside a stable boundary layer, and showed that the LLJ within the rotor area was eliminated due to the energy extraction and the enhanced mixing of momentum. Fitch et al. (2013) carried out simulations to quantify the impact of a WF covering 10×10 km on an ABL throughout a diurnal cycle using a mesoscale parameterization of the effects of WFs that include a momentum sink and a wind speed-dependent source of TKE. They found that the presence of a WF had a significant impact on the local atmospheric flow and on regions up to 60 km downwind at night, when the stable layer within the rotor area inhibited turbulent mixing of the momentum deficit, leading to a shallower wake and a greater reduction in the wind speed within the wake. It could completely eliminate the LLJ at altitudes within the rotor area.

One key scientific question is: How the 3D structure of the LLJ will be altered by the presence of large fields of spinning turbine rotors? To answer this question, we need to know how the WFs will modify major LLJ characteristics including the speed, height and amplitude, and the magnitude of the shear above and below the LLJ core. With the increase in the number of WTs installed and the diameter of the rotor and the height of the tower, the turbine-LLJ interactions will be more pronounced as more WTs reach deeper into the LLJ's typical height. It is expected that substantial deployment of WFs will show large-scale "waking" effects from many simultaneously spinning WTs within the LLJ envelope. Possibly there will be detectable degradation (or locally, complete elimination) of LLJ continuity within and downwind of the WFs, manifested by changes in the vertical structure and horizontal continuity of the wind field. Possibly, ABL stability and the strength, width and length of the LLJ will be changed due to their strong correlations. However, the effects of WFs on the occurrence, characteristics and evolution of the LLJ are largely unknown.

The LLJ plays a significant role in impacting regional precipitation, air quality, severe weather and climate events by transporting atmospheric moisture and constituents (Liu et al., 2014). Many studies have demonstrated strong relationships between LLJs and precipitation. In China, the LLJ is closely connected to torrential rainfall events and is a key indicator in rainfall prediction in China (Liu et al., 2014). The LLJ not only transports heat and moisture during precipitation, but also frequently stimulates the mesoscale fluctuation propagating along the jet core due to its strong instability. Also, its sharp wind shear can trigger mesoscale convective systems and thus lead to torrential rainfall events (Sun and Zhai, 1980). In the warm seasons, the Great Plains LLJ transports substantial amounts of warm, moist air from the Gulf of Mexico into the central US and provides low-level moisture convergence at its northern edges, facilitating the formation of thunderstorms and heavy precipitation (Barandiaran et al., 2013; Nikolic et al., 2019). Another relevant key question is how the WF-induced changes in the LLJs are manifested in weather and climate over and downwind of WFs? In particular, what's the impact on the transport of moisture and on precipitation patterns. However, the meteorological effects of WF-induced changes in LLJs, particularly on precipitation, are not known.

4.2 Large to global scale impacts

The local to regional impacts described above could collectively produce large to global scale impacts under the condition of the massive deployment of wind power. Evidently there are no observational work on this topic and so next we will focus on modeling studies.

4.2.1 Impacts on temperature and precipitation

Many GCM simulations using the enhanced roughness length parameterizations found significant WF impacts on weather and climate locally and remotely (e.g., Ivanova and Nadyozhina 2000; Keith et al. 2004; Kirk-Davidoff and Keith 2008; Barrie and Kirk-Davidoff 2010; Wang and Prinn 2010, 2011; Li et al., 2018). Next we summarize several representative GCM studies.

Keith et al. (2004) explored the possible regional and global impacts of the implementation of three approximately continent sized WFs using two GCMs. To simulate the added drag of the WFs, two parameterization schemes were employed. The first used perturbations to the drag coefficients over the installation regions. These perturbed drag coefficients were calculated by changing the surface roughness lengths over the WF areas. The other parameterization used an explicit drag scheme added to the model physics package in the two lowest model layers. Results pointed to a near negligible impact on globally average mean surface air temperatures but some WF regions experienced temperature changes of ± 2 °C in certain seasons, likely due to a shift of poleward heat transport. The changes in annual mean precipitation is less than 1% per terawatt (TW) and occurred mainly in northern mid- to high latitudes.

Wang and Prinn (2010) used a fully coupled atmosphere-ocean-land GCM to simulate the potential climate effects associated with installation of wind power to meet 10% or more of global energy demand in 2100. Seven model runs with 60-year durations were carried out. One run served as the control run, four runs used different parameterization schemes to represent the WT effects over land, and two runs used to represent installation of WFs in ocean depths shallower than 200 m between 60°S and 74°N. WT parameterizations over land included changing the model surface roughness and/or displacement height coefficients. Over the coastal installation areas, adding an additional surface drag component to the ocean surface parameterized the added friction imposed by the presence of WTs. The results showed surface warming exceeding 1 °C over land installations, but surface cooling

exceeding 1 °C over ocean installations. Significant warming or cooling remote from both the land and ocean installations, and alterations of the global distributions of rainfall and clouds also occurred. The rates of convective precipitation were generally reduced in the Northern Hemisphere and enhanced in the Southern Hemisphere. In the mid-latitudes, especially in the Northern Hemisphere, changes in large-scale precipitation also appeared, indicating an impact on mid-latitude weather systems. Although the changes in local convective and large-scale precipitation exceeded 10% in some areas, the global average changes were not very large.

Li et al. (2018) used a GCM with dynamic vegetation to show that large-scale installations of wind and solar farms, covering the Sahara at a scale large enough to power the entire world, had positive impacts. The effect of WTs was simply parameterized by changing the surface friction (drag coefficient) for easy implementation in the Earth system model framework and it was able to capture the first order WF impacts. The simulated WF impacts are most significant locally. The WFs caused significant regional warming on near-surface air temperature (+2.16 K), with greater changes in minimum temperature than maximum temperature (+2.36 vs. +1.85 K). They also led to more than twofold precipitation increase through increased surface friction and reduced albedo.

Recently, mesoscale models such as the WRF have been widely used to simulate and quantify WF impacts with more realistic WF deployment scenarios and better WT parameterizations. Next we summarize several representative studies using the WRF models.

Vautard et al. (2014) first quantified the regional climate effects of current wind energy production and a realistic wind energy development scenario across the whole of Europe in 2020 and found very limited WF impacts at the continental scale. They used the WRF model with the effects of WT being parameterized as the extraction of momentum and generation of additional TKE over the model layers containing the turbine blades. The simulation was integrated for 33 years with multiple sensitivity experiments being conducted. A statistically significant signal was only found in winter, with changes within ± 0.3 °C for temperature and within 0–5% for precipitation. Overall, the impacts remained much weaker than the natural climate interannual variability and changes expected from GHG emissions.

Miller and Keith (2018) used the WRF high-resolution regional model to quantify wind power's climate benefits and impacts at the continental scale. The WT parametrization of Fitch (2012) was adopted but customized for a Vestas 3-MW (MW) WT. They found that generating today's US electricity demand with wind power would warm continental US surface temperatures by 0.24 °C. Modeled diurnal and seasonal temperature differences were roughly consistent with observed WF warming effects. There was an overall 2% decrease of precipitation within the WF region but a large signal ranging between –50% and +50% outside the WF region toward the south-southwest direction. The warming effect was small compared with projections of 21st century warming, approximately equivalent to the reduced warming achieved by decarbonizing global electricity generation, and large compared with the reduced warming achieved by decarbonizing US electricity with wind. WF's overall environmental impacts were surely less than fossil energy.

Similarly, Huang et al. (2019) used the WRF simulations to examine the potential climatic impacts of four large-scale WF deployment scenarios in China, which represented small- (484 GW), medium- (2165 GW) and large-scale (3490 GW and 5412 GW) installed wind power capacities, respectively. The results showed that TKE, wind velocity, and air temperature varied consistently over the WFs with the largest changes in turbine hub heights. The large-scale WF scenarios could induce regional warming up to 0.8 °C in North China. The WF impacts on precipitation was insignificant.

Pryor et al. (2020) studied the climatic effects of doubling and quadrupling the installed capacity from the current 31 GW in the US using high-resolution (4 km) simulations with the WRF model. Theoretical scenarios for future deployments were based on repowering (i.e., replacing current WTs with newer, higher capacity WTs) to avoid competition for land. The results showed that WT-modified local near-surface climate (surface air temperature, specific humidity, precipitation and wind) was limited to the WT areas, was highly spatially variable, and exhibited important inter-annual variability. For example, the mean 2 m air temperature perturbation over the WF grid cells over the eastern US is –0.27 K, –0.18 K, and –0.03 K in summer, and +0.04 K, +0.06 K and +0.10 K in winter, for the current, doubled and quadrupled WF installed capacity, respectively. More modest impacts on precipitation were simulated, mainly during summer and fall. Median grid cell differences in total seasonal precipitation are <5 mm and <28 mm even in summer over WT grid cells (cf. domain-wide average of 428–450 mm). Overall, the precipitation perturbation was much smaller, spatially incoherent, and not robust to spatial averaging. Moreover, there was little spatial correlation with the location of WFs. The authors argued that the precipitation perturbation may reflect numerical noise rather than a systematic change in local or regional precipitation regime. In addition, this study concluded that climate impacts from the current and increased WT capacity scenarios were modest compared to regional changes induced by historical changes in land cover and to the global temperature perturbation induced by use of coal to generate an equivalent amount of electricity.

4.2.2 Impacts on wind patterns and large-scale circulation

Besides changes in temperatures and precipitation, both GCMs and WRF simulations showed that large WFs can modify wind patterns and circulation, which are often used to explain the WF-induced changes in weather and climate. Next, we will discuss several representative modeling studies using GCM and WRF.

Keith et al. (2004) found that atmospheric general circulations patterns were changed by the implementation of continent sized WFs. With a 10% increase of surface drag over land areas, mid-latitude average wind speeds decreased which caused the jet stream to shift poleward. This northward displacement of the location of the jet stream caused storms to track closer to the polar regions. Subsequently, this caused the high latitudes to cool and low latitudes to warm.

Kirk-Davidoff and Keith (2008) investigated the physical mechanisms of the simulated WF impacts on surface temperature, wind and cloud fraction in Keith et al. (2004) from the perspective of dynamical atmospheric processes. They used a simplified

GCM model to focus on the WF impacts upon the atmosphere without the influences of complex terrain seen in other GCMs. Large-scale WFs were parameterized by perturbations in surface roughness in central North America, Europe and East Asia as done in Keith et al. (2004). The magnitude and spatial pattern of surface air temperature change were quite similar to the results of Keith et al. (2004). The experiments showed a significant remote influence of large-scale roughness changes on synoptic scale winds and downstream storm tracks. The WF impacts occurred as a consequence of changes in the surface and tropospheric wind fields and general circulation, which, in turn resulted in advective heating and cooling, and change cloud fraction that influenced solar heating patterns. These changes modified the surface heat budget and caused the simulated temperature anomalies.

Barrie and Kirk-Davidoff (2010) used a GCM to represent a continent-scale WF in the central US and south-central Canada as a distributed array of surface roughness elements and indicated a strong downstream impact on short-term weather patterns. Their results showed that atmospheric anomalies initially developed at the WF site due to a slowing of the obstructed wind, propagated downstream as a variety of baroclinic and barotropic modes, and grew quickly when reaching the North Atlantic. The WF-induced perturbations involved substantial changes in the track and development of cyclones over the North Atlantic, and the magnitude of the perturbations rose above the level of forecast uncertainty.

Wang and Prinn (2010) indicated that the WF-induced changes in temperature, precipitation and clouds reflected an alteration to the large-scale circulation by the surface roughness changes caused by WTs. In particular, the changes in local convective and large-scale precipitation to a shift in the atmospheric Hadley Circulation.

Li et al. (2018) explained the WF-stimulated rainfall increase over the Sahel to the circulation changes associated with the warming-enhanced Saharan heat low through increased surface friction and reduced albedo. The increased surface friction reduced wind velocity and the associated Coriolis force, leading to a more dominant pressure gradient force toward the Saharan heat low that was enhanced by the WF-induced warming. This produced surface convergence and upward motion as well as moisture convergence and higher humidity. As expected, the increased drag at the surface due to WTs reduced wind speed by ~36%.

Vautard et al. (2014) showed in their WRF simulations that the changes in temperature and precipitation resulted from the combination of local WF effects and changes due to a weak, but robust, anticyclonic-induced circulation over Europe.

Huang et al. (2019) used the WRF simulations to examine the potential climatic impacts of four large-scale WF deployment scenarios in China, and attributed the large-scale WF-induced warming patterns to an anomalous circulation pattern with a negative pressure anomaly center in Northeast China and a positive pressure anomaly center in the middle and lower reaches of the Yangtze-Huaihe River Basin.

5 Ecological impacts of onshore wind farms

As discussed in Section 2.3, the WF-induced changes in microclimatic conditions could impact underlying vegetation and crops. Recent research work has detected ecological impacts due to operating WFs at local to regional scales, but the results are mixed.

5.1 Impacts on local vegetation cover

Construction of WFs over vegetated surfaces will result in the removal of vegetation associated with the turbine “footprint” within the WFs and thus reduce vegetation cover. However, the “footprint” area occupies only a small percentage of the total land area of WFs as discussed previously in Section 4.1.

Zhou et al. (2012) used MODIS data to detect changes in land use and vegetation cover over four large WFs over West-Central Texas, where the land use is mainly croplands. They found small and insignificant changes in land use and vegetation cover over the WFs and attributed these small changes to the turbine “footprint.”

Shen et al. (2017) mapped the damage of grasslands for a 10 million-kilowatt wind power base in Jiuquan City, Gansu Province, China. They performed an interactive interpretation of remote sensing images from the Landsat 8 and China’s GF-2 High-definition (GF-2) satellites and verified the accuracy of these interpretations using measured field data. Four regions of Yumen WFs covering a total area of 109.33 km² were selected and 354 pieces of WT equipment with an average construction density of 0.31 km² per device were evaluated. The construction of a single WT was found to damage nearly 3000 m² of grassland. The average area of grassland damaged by 3 MW and 1.5 MW turbines was 5757 m² and 2496 m², respectively. Roads covered 60.6% of the land occupied by wind power construction. The results indicated that WF construction did cause vegetation damage and other ecological problems. However, a total of ~2.44 km² of grassland was occupied by wind power construction and accounted for only ~2.2% of the study area.

5.2 Impacts on crop yields

Quantifying WF impacts on crop yields have important societal and economic implications, particularly in the Midwest and Great Plains where the WF growth rate is among the highest in the USA and WFs are often constructed over operating farmlands. A few studies indicated positive effects on crop yields.

To the best of our knowledge, the CWEX is so far the only comprehensive field campaign aiming to understand WF impacts on microclimate (e.g., momentum, heat, moisture and carbon dioxide) over croplands (Rajewski et al., 2013, 2014, 2016). It is reported that WFs modified heat, moisture flux and flow fields both above and below the turbine rotor layer and increased plant’s

transpiration at daytime as well as respiration at night, extending a few hundred meters downwind. Significant flux changes of CO₂, SM, and heat between downwind and upwind WF sites were detected. For example, fluxes of CO₂ and H₂O were enhanced by a factor of five in the leeward side of WTs during daytime. However, no actual measurements of plant activity over WFs are provided.

Rajewski et al. (2020) used measurements from a twin 120-m tall tower network in an agricultural landscape in Iowa to detect differences in the evening transition between a location outside of a large WF and near a single turbine or inside the WF. For a single WT, the wakes changed the onset of near-surface stabilization (earlier by a few hours), and lengthened the transition period (by up to an hour) within the rotor wake. For the multiple WTs in the WF, the aggregated wakes caused the differences in the transition of about ±30 min. The results provide additional evidence that WTs may influence biological regulation of soil microorganisms and plants within the WF.

Kaffine (2019) used a reduced-form, econometric approach to identify the microclimate effects of WFs on neighboring crop yields for the years 1997–2013. The study employed county-level crop and wind capacity data in the US to examine the effects of wind energy development on crop yields, controlling for time-invariant county characteristics and state-level annual shocks. This county-level data set was then matched with station-level meteorological data including daily precipitation, temperature, and surface wind from ~500 Automated Surface Observing System (ASOS) stations. Statistical approaches including the method of instrumental variables were used to estimate causal relationships and explore possible mechanisms. The results showed robust evidence that counties with increased wind power development also experienced increased corn yields, such that an additional 100 megawatts of wind capacity increase county yields by roughly 1%. Some evidence of similar effects was found for soy and hay yields, but not for wheat yields. Examination of other possible channels linking wind development and yields suggested that the WF-induced microclimate changes were likely main contributors to the higher crop yields.

Chen (2019) investigated the impacts of sizable WFs on local crop yields and agricultural activities based on the certified longitudinal farm-level data collected by the Illinois Farm Business Farm Management Association (FBFM) and the University of Illinois from 2003 to 2017, combined with the WT, weather and wind potential data. Statistical approaches including the method of instrumental variables (IV) were used to estimate causal relationships and explore possible mechanisms. The results showed that soybean and corn yields would increase by roughly 1.3% and 2.4%, respectively, given an additional 50 megawatts of wind capacity installed in the same county. Attribution analysis suggested that the WF-induced microclimate changes were likely main contributors to these increases as the development of wind energy had significant impacts on local meteorological variables.

5.3 Impacts on vegetation activity

Assessing the WF impacts on vegetation activity is an emerging new topic. There are a few studies using field observations and remote sensing data on this topic.

Pătru-Stupariu et al. (2019) investigated the WF impacts on plant communities in a mountain region. A field survey was conducted in a WF situated in the Southern Romanian Carpathians, 5 years after the turbines were installed. They tested for the effects of the presence of the turbine and the distance to the turbine on plant species richness, on five plant ecological indicators and on the quality of the pastures. Overall, 33 plant species belonging to 16 families were recorded, and among them 21 were recorded in both the presence and the absence of WTs. The presence of a turbine did not affect the structure of the plant community, as the majority of the plots exhibited similar plant species richness and composition. Finally, the values of the ecological indicators and the pasture quality were not altered by the presence of WTs either.

Xu et al. (2019) reported the positive ecological effects of large-scale WFs in Gobi ecosystems on vegetation at different scales using site experiments. The results indicated that under the influence of WTs, plants were more metabolically efficient, with higher community coverage, density, and aboveground biomass. A strong correlation was found between the changes in the community structure and the local climatic variations caused by the WTs.

Recently, there are several remote sensing studies to detect and quantify WF impacts on vegetation/crop growth using satellite observations. Satellite-based vegetation greenness indices (VIs) such as the enhanced vegetation index (EVI), leaf area index (LAI), and normalized difference vegetation index (NDVI) are direct optical measures of canopy greenness. They are highly correlated with plant photosynthesis and chlorophyll content and have been widely used to quantify vegetation dynamics and their responses to local meteorology change (Huete et al. 2002; Zhou et al., 2014). The methods of time series analysis and/or spatial pattern analysis (Section 3.1) are often used.

Li et al. (2016) used MODIS NDVI and other meteorological data to analyze the impact of wind direction on grassland vegetation over a 50 km buffer area around the Huitengliang WF in Inner Mongolia, China from 2000 to 2014. Compared with the construction phase (2000–2008), the operation phase (2008–2014) had a more obvious impact on vegetation growth. The results suggested that the WF impacts on vegetation were uneven and sensitive to wind direction: the WF was not conducive to vegetation growth within the WF area, while it was helpful to vegetation growth in windward/leeward areas.

Tang et al. (2017) used the MODIS VIs, MODIS primary productivity (gross primary production, GPP; net primary production, NPP), and other auxiliary data (temperature, soil moisture, evapotranspiration, albedo, and wind) to analyze possible WF effects on local vegetation growth in summer (June–August) from 2003 to 2014. The study area (40.9°N–41.5°N, 113.9°E–114.7°E) is located in the Bashang area of Hefei province, Northern China, and consists of 1747 WTs. The results showed that the WF had a significant inhibiting effect on vegetation growth and productivity, decreasing LAI, EVI and NDVI by approximately 14.5%, 14.8% and 8.9% from 2003 to 2014, respectively. The negative LAI differences between post- and pre-turbine periods (2012–2014 minus 2003–2005) were spatially coupled with the geographical layout of WTs. Similar results were also obtained from NDVI and EVI.

Both the spatial coupling and time series analyses provided clear observational evidences of the negative WF effect on vegetation growth. The WF-induced surface drying and water stress were proposed to explain such impacts.

Xia and Zhou (2017) conducted an extensive analysis of MODIS NDVI and EVI at 250 m resolution and meteorological data to investigate possible WF impacts on vegetation growth over two WF regions, one in West-Central Texas and the other in northern Illinois. These two regions differ in terms of land cover, topography, and background climate, and are well studied previously with significant local warming effects reported (Zhou et al. 2012; Slawsky et al. 2015). The results indicated that WFs had insignificant or no detectible impacts on local vegetation greenness. At the pixel level, the NDVI and EVI changes during the pre- and post-turbine periods demonstrated a random nature and have no spatial coupling with the WF layout. At the regional level, there was no systematic shift in vegetation greenness between the pre- and post-turbine periods. At interannual and seasonal time scales, there were no confident vegetation greenness changes over WFPs relative to NWFPs. Overall, there were some small decreases in VIs over WFPs, but no convincing observational evidence is found to be attributable to operating WFs.

So far, Li et al. (2018) is the only modeling study that discussed the WF impacts on vegetation. Their climate simulations showed that large-scale WF construction over the Sahara Desert could lead to increases in local vegetation coverage due to increased precipitation, and the resulting increase in vegetation further would enhance precipitation. This study demonstrated that the deployment of wind energy over deserts could have positive ecological impacts, as reported for the WFs in the Gobi ecosystems (Xu et al., 2019).

6 Major uncertainties

6.1 Observational uncertainties

There are mainly two types of uncertainties in the observational studies. The first results from the methods used to detect and quantify the WF impacts. The other is related to the uncertainties and errors in observational, reanalysis and remote sensed data.

It is challenging to isolate the WF contribution from the observed changes that contain both the WF and non-WF signals. For the observational methods used to detect the WF impacts (Section 3.1), the differences between two sites or two groups of pixels assume that they both share the same regional-scale background atmospheric signal, and so their differences remove the background signal and contain primarily the WF signal. However, this assumption is likely not true considering strong spatial variability due to land surface heterogeneity that is associated with variations in terrain, surface roughness, vegetation type and amount, and land cover/use. Similarly, the difference between two periods (pre- and post-WT periods) contains the background atmospheric change signal plus the WT impacts. The former changes every year following large-scale meteorological conditions, and could be estimated by empirical methods such as removing the regional interannual variability and using pixel level anomalies (Zhou et al., 2012, 2013a,b). However, these methods cannot completely eliminate this variability and thus introduce uncertainties into the detected WF signal.

It has been well established in the literature that all weather observations have some degree of uncertainty and errors, arising from several factors including changes in instrumentation, measurement practices, reporting, location and station environments (Philander, 2012). Reanalysis products result from the assimilation of observations from different sources into a state-of-the-art atmospheric model to produce a consistent and global data. However, changes in the observational type or coverage and errors in the assimilation systems can introduce artifacts and degrade the quality of the reanalyses (Torralba et al., 2017).

Similarly, remote sensing data also contain errors and inherent uncertainties (Loew et al., 2017). Satellite observations offers routine global coverage over extended periods (i.e., years), but most satellite data used for WF studies are derived from cloud-free scenes at a low revisit time (1–2 *daily* passes). The resulting data gaps create inhomogeneity in compositing geospatial images, and the coarse spatial and temporal resolutions cannot capture the time evolution of small-scale turbine effects. In addition, remote sensing data also contain uncertainties due to residual atmospheric effects from clouds and aerosols and errors from observations and retrievals (Wan, 2006). Furthermore, different data processing methods have been developed to remove artifacts associated with satellite drift, sensor degradation and residual atmospheric effects, and resulted in differences, particular at local to regional scales. For example, Xia and Zhou (2017) found insignificant or no detectible WF impacts on vegetation growth in two US WFs, while Tang et al. (2017) indicated a significant inhibiting effect on vegetation growth in a Chinese WF. It is worth noting that the background state of vegetation greenness in Texas is very similar to that examined in Tang et al. (2017), and identical approaches were used. This inconsistency, however, could partially result from the differences in the data used: Xia and Zhou (2017) used the MODIS Collection 6 vegetation greenness product while Tang et al. (2017) used the MODIS Collection 5 data. MODIS data suffered from sensor degradation that was not well corrected in the MODIS Collection 5 datasets (Heck et al., 2019). It is also possible that the WF impacts on vegetation differ largely by region due to differences in the background environmental factors, such as temperature, moisture and land properties (Tang et al., 2017).

6.2 Modeling uncertainties

There are mainly two types of uncertainties in the modeling studies. The first depends on numerical models' credential in simulating local to regional meteorology. The other is related to the model capability in realistically characterizing the WT-atmosphere-surface interactions in the WT parametrizations.

Regional or global models represent WT effects with subgrid-scale parameterizations. Their capabilities of simulating WF impacts depend strongly on the credentials of the models employed to simulate the background atmospheric conditions and of the WT parameterization schemes applied to simulate the WT effects (Pryor et al., 2018, 2020).

Weather and climate models are largely based on mathematical representations of the earth system processes governed by the laws of physics. Current WF impact studies are built primarily on numerical simulations with regional and global models. Numerical models allow us to simulate spatial and temporal patterns of near-surface ABL, meteorological fields, and surface fluxes within and around WFs. Realistically describing exchanges of energy, momentum, mass, moisture, and trace gases between the surface and the atmosphere in the ABL are crucial in simulating land-atmosphere coupling and interactions. However, it is well known that numerical models have large uncertainties in simulating local to regional weather and climate due to coarse resolution, particularly over complex terrain (IPCC, 2007a,b; Slingo and Palmer, 2011).

It has become clear from recent studies that despite many improvements and updates, current WT parameterization schemes still have large limitations and uncertainties in accurately describing the complex WF-ABL-surface interactions. In particular, due to lack of observations, WT parameterizations have not been well validated (Baidya Roy and Traiteur 2010; Zhou et al., 2012, 2013a,b; Xia et al., 2017, 2019). For example, Fitch et al. (2013) examined the differences of WF effects on local microclimate using current WT parameterization schemes and concluded that the increased surface roughness approach is inappropriate for representing WFs because it leads to very different atmospheric responses from the mesoscale approaches, which are closer to observations. Zhang et al. (2013) conducted well-controlled wind-tunnel experiments to understand the WF-atmosphere interactions for large-scale WFs and suggested that it is essential to simulate the wake rotation effects in numerical models of WF flows in order to reproduce the spatial distribution of the surface heat flux. Without simulating the wake rotation effects, turbulent mixing might be underestimated in the wake, resulting in incorrectly simulated momentum and heat transport near the surface as shown in the increased surface roughness approaches used in GCMs. Considering real-world WFs and the latest WT parameterization, Xia et al. (2017, 2019) showed that the WRF model is moderately successful at reproducing the observed LST variations over West-Central Texas. However, they also produced a strong downwind cooling effect that is not seen in observations and satellites. Wisser et al. (2011) argued that: (1) the WT schemes may not accurately represent the mechanisms by which how WTs actually interact with the atmosphere; (2) it is often incorrectly assumed that WTs act as invariant momentum sinks, turbine densities are above what is the norm, and wind energy deployment occurs at a more substantial and geographically concentrated scale than is likely. These issues will likely introduce large uncertainties in simulated WF impacts.

7 Future work

Here we suggest an increase in research effort in the following fields.

More field campaigns. The best way to assess the WF impacts will be to conduct a series of extensive field campaigns in operating WFs under various meteorological and terrain conditions and WF configurations. The field campaigns should be designed such that they simultaneously collect information about wake turbulence, micrometeorology and synoptic scale meteorology over WFs and surrounding regions. This will require simultaneous deployment of Lidars in WT wakes, surface weather stations and meteorological towers upwind and downwind of WTs, as well as advanced weather radars, and sensors from airborne platforms. These measurements can be used to improve WT parameterizations, evaluate model results, and advance our understanding of the WT-ABL-surface interactions.

More high-resolution remote sensing studies. As field campaigns are expensive and can only be run for a short time, another useful approach is to analyze high-resolution remote sensing data. Satellites and radars provide information of regional to global spatial sampling at regular temporal intervals and thus have the potential to accurately monitor and detect impacts of large WFs with spatial detail. They could be the most cost-effective and fastest approaches at this stage, allowing us to identify impacts of WFs over a wider range of spatiotemporal scales than typical field campaigns. For example, a series of remote sensing studies discussed previously present observational evidence of WF impacts. Most importantly, the knowledge obtained from such studies will also offer guidance to future field campaign organizers about the optimal selection and deployment of instruments and the optimal location and timing of planned field campaigns.

More realistic WT parameterization schemes. Realistically describing the dynamic and thermodynamic processes in the WT-atmosphere-surface interface into numerical models is the foundation of assessing potential WF impacts. The scientific community needs to evaluate how well current models represent local to regional meteorology, and to examine whether the WT parameterizations are sufficiently advanced to represent the complex WT-ABL-surface interactions. Improving WT parameterizations and validating model results against observations should be a top priority. The availability of high-quality remote sensed data such as MODIS at 250 m to 1 km resolutions, in situ observations and near-surface meteorological fields, and reanalysis data could be compared with the model results. More effort should be put to identify the models that can best simulate local to regional weather and climate processes and couple the identified models with the WT parameterizations that can best describe the WT-atmosphere-surface processes.

More process-based studies for realistic WFs. Given our limited knowledge of WT-atmosphere-surface interactions and large uncertainties in simulating and projecting the impacts of WFs, it is essential to conduct more comprehensive process-based studies to detect and quantify the weather, climatic and ecological impacts of realistic WFs under different meteorological, terrain and land surface conditions. Combining both observational and modeling frameworks will reduce the uncertainties of results and enhance

the confidence and robustness of findings. In particular, the availability of various observations (near-surface meteorological variables, radar and remote sensed) and reanalysis data can be used, not only to detect, quantify and attribute potential WF impacts, and but also to validate the model results. It is fundamental to understand the detailed physical processes of how WFs change the diurnal, seasonal and interannual variations of ABL structures and near-surface hydrometeorology, and how these changes vary across a wide range of hosting landscapes globally and under different WF configurations.

More research on WF-vegetation interactions. We particularly call for more observational studies from field campaigns and remote sensing to improve our understanding of vegetation-WF interactions. One key question is how WF-induced changes in microclimate may modify plant growth, phenology, and productivity? Current research is limited to short-term WF impacts on crop yields and vegetation activity. However, the influences of WFs on ecosystems depends on species and location (Armstrong et al., 2014) and plant's responses to microclimate change varies with time scale and background climate (Xu et al., 2019). Considering collocation of WFs with crops and vegetation, it is necessary to examine potential long-term effects on different ecosystems and integrate with other environmental factors such as microclimatic conditions or soil properties (Xu et al., 2019). More effort is also needed to model vegetation dynamics and vegetation responses and feedbacks to WF-induced changes.

More research on WF-LLJ interactions. As discussed previously, the LLJ plays a significant role in impacting regional precipitation, severe weather and climate events by transporting atmospheric heat, moisture and constituents. Given the projected large installation in wind energy in the Midwest and Great Plains, it is important to use observations and models to address two key questions: (1) how the WFs impact the occurrence, characteristics and evolution of the Great Plains LLJs? and (2) how the WF-induced changes in the Great Plains LLJs affect weather and climate, in particular, precipitation patterns, over and downwind of WFs?

8 Conclusion and discussion

This chapter reviews our current knowledge of potential weather, climatic and ecological impacts of WFs. The main findings can be summarized as follows.

8.1 Key summary

Wind turbine wake effects: There is a general consensus from observations and modeling studies that operating WTs reduce the wind speed behind the turbines, and also increase vertical mixing by introducing turbulence across a range of length scales. WFs affect the atmosphere and the land surface because they act as both a sink of the wind's kinetic energy and as a source of turbulence.

Impacts on temperatures: There is a general consensus from observations and modeling studies that operating WFs produce a local warming effect at night but a small and insignificant effect at day. This asymmetric warming effect results from the turbine-enhanced vertical turbulent mixing in the wakes. Typically, nighttime has a shallow and stable ABL with a warm layer overlying a cool layer and cold ground. The turbine-enhanced vertical mixing mixes warm air down and cold air up, leading to a warming near the surface. Daytime often has an unstable atmosphere with cool air lying over warmer air. Turbulent wakes mix cool air down and warm air up, producing a cooling near the surface. However, the daytime mixing in the background atmosphere is already very large due to solar heating. Hence, the turbine-enhanced turbulent mixing plays a minimal role during the daytime. The warming effect is generally local. At local to regional scales, the magnitude of warming could be significant, but the global mean effects seem to be small.

Impacts on precipitation: A few modeling studies show that WFs modify precipitation either over WFs locally or downwind remotely, although the magnitude, sign and spatial patterns vary by location and time. There is no consensus on the effects of WFs on precipitation. It is challenging to detect and quantify the WF-induced precipitation signatures using observations. Isolating the WF impacts on precipitation is perhaps possible only in models, not in observations.

Impacts on wind patterns: Both observations and models show that the presence of WTs modifies the 3D inflow conditions in the rotor-swept area, the wind shear and turbulence in and downwind of WTs. A few modeling studies show that WTs may impact low level jets and regional to large-scale circulation, but there is no consensus on such impacts.

Impacts on vegetation: A few observational studies reported positive WF impacts on crop yields, but mixed results on vegetation activity overall. There is no consensus on such impacts. Among the WF-induced microclimate effects, some could be beneficial to vegetation and some may be harmful for plant activity.

WFs interact with the atmosphere because they act as both a sink of the wind's kinetic energy and as a source of turbulence induced by the rotor blades. Inevitably, they enhance vertical mixing of ABL and thus modify surface heat and moisture fluxes, which influence surface temperature, moisture, energy fluxes and atmospheric stability. WFs add friction to the flow, which reduces wind speeds in the turbine wake areas and changes wind patterns. These local changes, if spatially large enough, can collectively modify precipitation, radiation, clouds, atmospheric general circulations, and heat and moisture advection, which could produce noticeable effects on weather and climate locally and remotely (Traiteur and Baidya Roy, 2011).

A large number of studies using both models and observations have documented potential WFs on weather and climate system. While the WF-induced changes on temperatures have been intensively studied, the impacts on precipitation, wind patterns, clouds, and vegetation in and downwind of WFs remains with large uncertainty, are region specific and scale dependent. Large and significant impacts at local to regional scales, particularly on temperature, have been reported. In contrast, the global impacts of very large wind energy deployment are modest, only significant at certain regions and certain seasons. Despite small global impacts, the

local changes in microclimate due to operating WT's could have implications for ecosystems and human activities (Armstrong et al., 2014).

8.2 Relative to other man-made climate impacts

It is important to recognize that the build-up of CO₂ in the atmosphere due to the burning of fossil fuels has global and long-term impacts, whereas impacts of WFs are mostly local (confined to the WF areas) and short-term (absent if the WT's are turned off). Also, WT's don't produce any heat but simply vertically redistribute the heat that is already in the atmosphere, which is fundamentally different from the large-scale cumulative greenhouse warming effect due to increasing GHGs. Renewable wind energy reduces GHG emissions and thus mitigates global warming. Furthermore, the reported long-term environmental impacts of massive WF deployment are generally more regional in space and smaller in magnitude, than the natural climate interannual variability and changes expected from fossil fuels and historical land cover/use (Wang and Prinn, 2010; Vautard et al., 2014; Miller and Keith, 2018; Li et al., 2018; Pryor et al., 2020).

8.3 Final remarks

All energy sources have some impacts on our environment, but fossil fuels do substantially more damage than renewable wind energy—air and water pollution, damage to public health, wildlife and habitat use, water use, land use and global warming emissions (UCS, 2013). In comparison, wind power is an environmentally sustainable, with minimal effects and is likely to be part of the solution to the climate change, air pollution, and energy security problems.

Assessing potential WF impacts is critical for developing efficient adaptation and management strategies to ensure long-term sustainability of wind power. Increasing scientific and public interests in assessing environmental consequences of WFs highlight the need to: (1) understand the detailed dynamic and thermodynamic processes due to operating WFs and how these changes modify surface properties and boundary layer meteorology, and eventually affect weather, climate, and vegetation activity; (2) develop and improve numerical models that can realistically characterize WT-atmosphere-surface interactions to assess potential WF impacts.

Given the spatial scale of installed and projected wind power, WF impacts should be assessed in detail as part of all future climate change assessments, in order for them to be scientifically complete. This includes not only local effects within and around WFs, but also their roles in altering large to global scale climate and circulations remotely (Mahmood et al., 2010). However, the influence of WFs on climate and weather is extremely complex, and our current understanding of WT-ABL-surface interactions are still very limited. More studies are needed to improve our knowledge of these interactions and our capacity to model and project WF impacts on weather, climate, water cycle and ecosystems.

References

- Abkar M and Porté-Agel F (2015) A new wind-farm parameterization for large-scale atmospheric models. *Journal of Renewable and Sustainable Energy* 7: 013121.
- Adams AS and Keith DW (2013) Are global wind power resource estimates overstated? *Environmental Research Letters* 8: 015021.
- Ancell BC, Bogusz A, Lauridsen MJ, and Nauert CJ (2018) Seeding chaos: The dire consequences of numerical noise in NWP perturbation experiments. *Bulletin of the American Meteorological Society* 99: 615–628.
- Armstrong A, Waldron S, Whitaker J, and Ostle NJ (2014) Wind farm and solar park effects on plant-soil carbon cycling: Uncertain impacts of changes in ground-level microclimate. *Global Change Biology* 20: 1699–1706.
- Armstrong A, Burton RR, Lee SE, Mobbs S, Ostle N, Smith V, and Whitaker J (2016) Ground-level climate at a peatland wind farm in Scotland is affected by wind turbine operation. *Environmental Research Letters* 11: 044024.
- Baidya Roy S (2011) Simulating impacts of wind farms on local hydrometeorology. *Journal of Wind Engineering and Industrial Aerodynamics* 99: 491–498.
- Baidya Roy SB and Traiteur JJ (2010) Impact of wind farms on surface air temperatures. *Proceedings of the National Academy of Sciences of the United States of America* 107: 17899–17904.
- Baidya Roy S, Pacala SW, and Walko RL (2004) Can large wind farms affect local meteorology? *Journal of Geophysical Research* 109: D19101.
- Baker RW and Walker SN (1984) Wake measurements behind a large horizontal axis wind turbine generator. *Solar Energy* 33: 5–12.
- Barandiaran D, Wang S-Y, and Hilburn K (2013) Observed trends in the Great Plains low-level jet and associated precipitation changes in relation to recent droughts. *Geophysical Research Letters* 40: 6247–6251.
- Barrie D and Kirk-Davidoff DB (2010) Weather response to a large wind turbine array. *Atmospheric Chemistry and Physics* 10: 769–775.
- Barthelmie R, Larsen G, Pryor S, Jørgensen H, Bergström H, Schlez W, Rados K, Lange B, Volund P, Neckelmann S, Mogensen S, Schepers G, Hegberg T, Folkerts L, and Magnusson M (2004) ENDOW (efficient development of offshore windfarms): Modelling wake and boundary layer interactions. *Wind Energy* 7: 225–245.
- Bjornsson H and Venegas SA (1997) A manual for EOF and SVD analyses of climatic data. In: *McGill University CCGCR Rep. 97-1*. 54 pp. [Available online at <http://www.geog.mcgill.ca/gec3/wp-content/uploads/2009/03/Report-no.-1997-1.pdf>].
- Blahak U, Goretzki B, and Meis J (2010) A simple parameterization of drag forces induced by large wind farms for numerical weather prediction models. In: *Proc. European Wind Energy Conf. and Exhibition 2010, PO ID 445, Warsaw, Poland, EWEC* 186–189.
- Bloomberg New Energy Finance (BNEF), 2019 New Energy Outlook 2019. <https://about.bnef.com/new-energy-outlook/>.
- Bonner WD (1968) Climatology of low level jet. *Monthly Weather Review* 96: 833–850.
- Cai X, Gu R, Pan P, and Zhu J (2016) Unsteady aerodynamics simulation of a full-scale horizontal axis wind turbine using CFD methodology. *Energy Conversion and Management* 112: 146–156.
- Calaf M, Parlange M, and Meneveau C (2011) Large eddy simulation study of scalar transport in fully developed wind-turbine array boundary layers. *Physics of Fluids* 23: 126603.
- Carroll BJ, Demoz BB, and Delgado R (2019) An overview of low-level jet winds and corresponding mixed layer depths during PECAN. *Journal of Geophysical Research-Atmospheres* 124: 9141–9160.

- Cervarich MC, Baidya Roy S, and Zhou L (2013) Spatiotemporal structure of wind farm-atmospheric boundary layer interactions. *Energy Procedia* 40: 530–536.
- Chang R, Zhu R, and Guo P (2016) A case study of land-surface-temperature impact from large-scale deployment of wind farms in China from Guazhou. *Remote Sensing* 8: 790.
- Chen T (2019) Wind energy and agricultural production—Evidence from farm-level data. In: *2019 Annual Meeting, July 21–23, Atlanta, Georgia 291222, Agricultural and Applied Economics Association*. Handle: RePEC:ags:aaea19:291222.
- Christiansen MB and Hasager CB (2005) Wake effects of large offshore wind farms identified from satellite SAR. *Remote Sensing of Environment* 98: 251–268.
- Churchfield MJ, Lee S, Michalakes J, and Moriarty PJ (2012) A numerical study of the effects of atmospheric and wake turbulence on wind turbine dynamics. *Journal of Turbulence* 13: 1–32.
- Clifton A, Schreck S, Scott G, Kelley N, and Lundquist JK (2013) Turbine inflow characterization at the National Wind Technology Center. *Journal of Solar Energy Engineering* 135: 031017.
- Du Y, Rotunno R, Zhang Q, Chen YL, and Yin W (2016) The characteristics and formation mechanisms of low level jets in China and their relationship with wind energy. In: *Seventh Conference on Weather, Climate, Water and the New Energy Economy, AMS 96th Annual Meeting, 2016*. <https://ams.confex.com/ams/96Annual/webprogram/Paper284580.html>.
- Fiedler BH and Bukovsky MS (2011) The effect of a giant wind farm on precipitation in a regional climate model. *Environmental Research Letters* 6: 045101.
- Fitch AC, Olson JB, Lundquist JK, Dudhia J, Gupta AK, Michalakes J, and Barstad I (2012) Local and mesoscale impacts of wind farms as parameterized in a mesoscale NWP model. *Monthly Weather Review* 140: 3017–3038.
- Fitch AC, Olson JB, and Lundquist JK (2013) Parameterization of wind farms in climate models. *Journal of Climate* 26: 6439–6458.
- Frandsen S (1992) On the wind speed reduction in the center of large clusters of wind turbines. *Journal of Wind Engineering and Industrial Aerodynamics* 39: 261–265.
- Freedman JM, Flores I, Zack J, Schroeder J, Ancell B, Brewster K, Basu S, Banunaryanan V, and Ela E (2014) The wind forecast improvement project (WFIP): A public/private partnership for improving short term wind energy forecasts and quantifying the benefits of utility operations—The southern study area. In: *AWS Truepower Final Technical Report to DOE, award number DE-EE0004420*. 107 pp. Available online at <http://www.osti.gov/scitech/biblio/1129905>.
- Gallo KP and Owen TW (1999) Satellite-based adjustments for the urban heat island temperature bias. *Journal of Applied Meteorology* 38: 806–813.
- Global Wind Energy Council (GWEC) (2019) China Wind Power 2019. <https://gwec.net/china-wind-power-2019/>.
- Harris RA, Zhou L, and Xia G (2014) Satellite observations of wind farm impacts on nocturnal land surface temperature in Iowa. *Remote Sensing* 6: 12234–12246.
- Heck E, de Beurs KM, Owsley BC, and Henebry GM (2019) Evaluation of the MODIS collections 5 and 6 for change analysis of vegetation and land surface temperature dynamics in north and South America. *ISPRS Journal of Photogrammetry and Remote Sensing* 156: 121–134.
- Huang J-B, Lou P-K, Sun H-W, Luo Y, and Zhao Z-C (2019) Numerical experimental study on the potential climatic impacts of large-scale wind farms in China. *Advances in Climate Change Research* 10: 143–149.
- Huete A, Didan K, Miura T, Rodriguez EP, Gao X, and Ferreira LG (2002) Overview of the radiometric and biophysical performance of the MODIS vegetation indices. *Remote Sensing of Environment* 83(1-2): 195–213.
- IPCC (2007a) *Climate Change 2007: Impacts, Adaptation and Vulnerability. Contribution of Working Group II to the Fourth Assessment Report of the Intergovernmental Panel on Climate Change*. Cambridge, UK: Cambridge University Press.
- IPCC (2007b) *Climate Change 2007: The Physical Science Basis. Contribution of Working Group I to the Fourth Assessment Report of the Intergovernmental Panel on Climate Change*. Cambridge, United Kingdom and New York, NY, USA: Cambridge University Press.
- Itskos G, Nikolopoulos N, Kourkoumpas D-S, Koutsianos A, Violidakis I, Drosatos P, and Grammelis P (2016) *Environment and Development: Basic Principles, Human Activities, and Environmental Implications*. Elsevier. ISBN: 978-0-444-62733-9363–452.
- Ivanova LA and Nadyozhina ED (2000) Numerical simulation of wind farm influence on wind flow. *Wind Engineering* 24: 257–270.
- Jacobson MZ and Archer CL (2012) Saturation wind power potential and its implications for wind energy. *Proceedings of the National Academy of Sciences of the United States of America* 109(15): 679–15,684.
- Jawaheer BO, Dhunny AZ, Cunden TSM, Chandrasekaran N, and Lollchund MR (2019) Modelling the effects of wind farming on the local weather using weather research and forecasting (WRF) model. In: Satapathy S, Bhateja V, Somanah R, Yang XS, and Senkerik R (eds.) *Information systems design and intelligent applications. Advances in intelligent systems and computing*. vol. 863. Singapore: Springer.
- Kaffine DT (2019) Microclimate effects of wind farms on local crop yields. *Journal of Environmental Economics and Management* 96: 159–173.
- Kalnay E and Cai M (2003) Impact of urbanization and land-use change on climate. *Nature* 423: 528–531.
- Keith DW, DeCarolis JF, Denkenberger DC, Lenschow DH, Malyshev SL, Pacala S, and Rasch PJ (2004) The influence of large-scale wind power on global climate. *Proceedings of the National Academy of Sciences of the United States of America* 101: 16115–16120.
- Kirk-Davidoff DB and Keith DW (2008) On the climate impact of surface roughness anomalies. *Journal of the Atmospheric Sciences* 65: 2215–2234.
- Lauridsen MJ and Ancell BC (2018) Nonlocal inadvertent weather modification associated with wind farms in the Central United States. *Advances in Meteorology* 2018: 2469683.
- Lee JCY and Lundquist JK (2017) Evaluation of the wind farm parameterization in the weather research and forecasting model (version 3.8.1) with meteorological and turbine power data. *Geoscientific Model Development* 10: 4229–4244.
- Li G, Zhang CH, Zhang L, and Zhang M (2016) Wind farm effect on grassland vegetation due to its influence on the range, intensity and variation of wind direction. In: *IEEE International Geoscience and Remote Sensing Symposium* 1304–1306.
- Li Y, Kalnay E, Motesharrei S, Rivas J, Kucharski F, Davidoff DF, Bach E, and Zeng N (2018) Climate model shows large-scale wind and solar farms in the Sahara increase rain and vegetation. *Science* 361: 1019–1022.
- Liu H, He M, Wang B, et al. (2014) Advances in low-level jet research and future prospects. *Journal of Meteorological Research* 28: 057–075.
- Loew A, Bell W, Brocca L, Bulgin CE, Burdanowitz J, Calbet X, Donner RV, Ghent D, Gruber A, Kaminiski T, Kinzel J, Klepp C, Lambert JC, Strub-Schaepman G, Schöder M, and Verhoelst T (2017) Validation practices for satellite-based Earth observation data across communities. *Reviews of Geophysics* 55: 779–817.
- Lu H and Porté-Agel F (2011) Large-eddy simulation of a very large wind farm in a stable atmospheric boundary layer. *Physics of Fluids* 23: 065101.
- Lu M, Zhou X, and Luo Y (2013) Responses of ecosystem carbon cycle to experimental warming: A meta-analysis. *Ecology* 94: 726–738.
- Lundquist JK, DuVivier KK, Kaffine D, and Tomaszewski JM (2019) Costs and consequences of wind turbine wake effects arising from uncoordinated wind energy development. *Nature Energy* 4: 26–34.
- Mahmood R, Pielke RA Sr., Hubbard KG, Niyogi D, Bonan G, Lawrence P, McNider R, McAlpine C, Etter A, Gameda S, and Qian B (2010) Impacts of land use/land cover change on climate and future research priorities. *Bulletin of the American Meteorological Society* 91: 37–46.
- Martino J (2014) *Advancements in Wind Turbine Technology: Improving Efficiency and Reducing Cost*. USA: Power Engineering. Retrieved Section 9.10.2.3.7, 2020. <https://www.renewableenergyworld.com/2014/04/02/advancements-in-wind-turbine-technology-improving-efficiency-and-reducing-cost/#gref>.
- Marvel K, Kravitz B, and Caldeira K (2013) Geophysical limits to global wind power. *Nature Climate Change* 3: 118–121.
- McNaughton KG (1988) Effects of windbreaks on turbulent transport and microclimate. *Agriculture, Ecosystems and Environment* 22–23: 17–39.
- Meyers M and Meneveau C (2012) Optimal turbine spacing in fully developed wind farm boundary layers. *Wind Energy* 15: 305–317.
- Miller LM and Keith DW (2018) Climatic impacts of wind power. *Joule* 2: 2618–2632.
- Moomaw W, Yamba F, Kamimoto M, Maurice L, Nyboer J, Urama K, and Weir T (2011) Introduction. In: Edenhofer O, Pichs-Madruga R, Sokona Y, Seyboth K, Matschoss P, Kadner S, ... von Stechow C (eds.) *IPCC Special Report on Renewable Energy Sources and Climate Change Mitigation*. Cambridge, United Kingdom and New York, NY, USA: Cambridge University Press.
- Moravec D, Barták V, Puš V, and Wild J (2018) Wind turbine impact on near-ground air temperature. *Renewable Energy* 123: 627–633.
- Nikolic J, Zhong S, Bian X, Heilman WE, and Charney JJ (2019) Sensitivity of low-level jets to land-use and land-cover change over the continental U.S. *Atmosphere* 10: 174.

- Pan Y and Archer CL (2018) A hybrid wind-farm parametrization for mesoscale and climate models. *Boundary-Layer Meteorology* 168: 469–495.
- Pătru-Stupariu I, Calotă A, Santonja M, Anastasiu P, Stoicescu I, Biris IA, Stupariu MS, and Buttler A (2019) Do wind turbines impact plant community properties in mountain region? *Biologia* 74: 1613–1619.
- Petersen EL, Mortensen NG, Landberg L, Højstrup J, and Frank HP (1998) Wind power meteorology. Part I: Climate and turbulence. *Wind Energy* 1: 25–45.
- Peterson TC (2003) Assessment of urban versus rural in situ surface temperatures in the contiguous United States: No difference found. *Journal of Climate* 18: 2941–2959.
- Philander SG (ed.) (2012) *Encyclopedia of Global Warming and Climate Change*. 2nd edn., In: vol. 1, p. 1720. SAGE Publications, Inc.
- Prasad B, Carver BF, Stone ML, Babar MA, Raun WR, and Klatt AR (2007) Potential use of spectral reflectance indices as a selection tool for grain yield in winter wheat under great plains conditions. *Crop Science* 47: 1426–1440.
- Pryor SC, Barthelme RJ, and Shepherd TJ (2018) The influence of real-world wind turbine deployments on local to mesoscale climate. *Journal of Geophysical Research – Atmospheres* 123: 5804–5826.
- Pryor SC, Barthelme RJ, and Shepherd TJ (2020) 20% of US electricity from wind will have limited impacts on system efficiency and regional climate. *Scientific Reports* 10: 1–14.
- Rajewski DA, Takle ES, Lundquist JK, Oncley S, Prueger JH, Horst TW, Rhodes ME, Pfeiffer R, Hatfield JL, Spoth KK, and Doorenbos RK (2013) Crop wind energy experiment (CWEX): Observations of surface-layer, boundary layer, and mesoscale interactions with a wind farm. *Bulletin of the American Meteorological Society* 94: 655–672.
- Rajewski DA, Takle ES, Lundquist JK, Prueger JH, Pfeiffer RL, Hatfield JL, Spoth KK, and Doorenbos RK (2014) Changes in fluxes of heat, H₂O, and CO₂ caused by a large wind farm. *Agricultural and Forest Meteorology* 194: 175–187.
- Rajewski DA, Takle ES, Prueger JH, and Doorenbos RK (2016) Toward understanding the physical link between turbines and microclimate impacts from in situ measurements in a large wind farm. *Journal of Geophysical Research – Atmospheres* 121: 13392–13414.
- Rajewski DA, Takle ES, VanLoocke A, and Purdy SL (2020) Observations show that wind farms substantially modify the atmospheric boundary layer thermal stratification transition in the early evening. *Geophysical Research Letters*. <https://doi.org/10.1029/2019GL086010>.
- Reedern S, Olson JB, Lundquist JK, and Clack CTM (2019) Incorporation of the rotor-equivalent wind speed into the weather research and forecasting model's wind farm parameterization. *Monthly Weather Review* 147: 1029–1046.
- Rhodes ME and Lundquist JK (2013) The effect of wind turbine wakes on summertime Midwest atmospheric wind profiles. *Boundary-Layer Meteorology* 149: 85–103.
- Roser M (2020) *Economic Growth*. Published online at OurWorldInData.org. Retrieved from: <https://ourworldindata.org/economic-growth> [Online resource].
- Shen G, Xu B, Jin Y, Chen S, Zhang W, Liu H, Zhang Y, and Yang X (2017) Monitoring wind farms occupying grasslands based on remote-sensing data from China's GF-2 HD satellite—A case study of Jiuquan City, Gansu province, China. *Resources, Conservation and Recycling* 121: 128–136.
- Skamarock WC and Klemp JB (2008) A time-split nonhydrostatic atmospheric model for weather research and forecasting applications. *Journal of Computational Physics* 227: 3465–3485.
- Skamarock WC, et al. (2008) *A Description of the Advanced Research WRF version 3*. Tech. Rep. NCAR/TN-475+STR. University Corporation for Atmospheric Research 113.
- Slawsky LM, Zhou L, Baidya Roy S, Xia G, Vuille M, and Harris RA (2015) Observed thermal impacts of wind farms over Northern Illinois. *Sensors* 15: 14981–15005.
- Slingo J and Palmer T (2011) Uncertainty in weather and climate prediction. *Philosophical Transactions. Series A, Mathematical, Physical, and Engineering Sciences* 369: 4751–4767.
- Smith CR, Barthelme RJ, and Pryor SC (2013) In situ observations of the influence of a large onshore wind farm on near-surface temperature, turbulence intensity and wind speed profiles. *Environmental Research Letters* 8: 034006.
- Snyder RL and de Melo-Abreu JP (2005) *Frost Protection: Fundamentals, Practice and Economics*. Environmental and Natural Resources Series, vol. 1. Rome: FAO.
- Stull RB (1988) *An Introduction to Boundary Layer Meteorology*. Dordrecht: Kluwer. 666 pp.
- Sun SQ and Zhai GQ (1980) On the instability of the low level jet and its trigger function for the occurrence of heavy rainstorms. *Chinese Journal of Atmospheric Sciences* 4: 327–337.
- Tang B, Wu D, Zhao X, Zhou T, Zhao W, and Wei H (2017) The observed impacts of wind farms on local vegetation growth in northern China. *Remote Sensing* 9: 332.
- The U.S. Energy Information Administration (EIA) (2019) Wind Explained: History of Wind Power. <https://www.eia.gov/energyexplained/wind/history-of-wind-power.php>. April 4, 2019.
- Torraiba V, Doblas-Reyes FJ, and Gonzalez-Reviriego N (2017) Uncertainty in recent near-surface wind speed trends: A global reanalysis intercomparison. *Environmental Research Letters* 12: 114019.
- Traiteur J and Baidya Roy S (2011) Chapter 8: Impacts of wind farms on weather and climate at local and global scales. In: Lehr JH, Keeley J, and Kingery TB (eds.) *Alternative Energy and Shale Gas Encyclopedia*, First published: 22 April 2016, Online ISBN: 9781119066354. Print ISBN: 9780470894415.
- Union of Concerned Scientists (UCS) (2013) Environmental Impacts of Renewable Energy Technologies. Published Jul 14, 2008 Updated Mar 5, 2013. <https://www.ucsusa.org/resources/environmental-impacts-renewable-energy-technologies>.
- Vanderwende BJ, Kosović B, Lundquist JK, and Mirocha JD (2016) Simulating effects of a wind-turbine array using LES and RANS. *Journal of Advances in Modeling Earth Systems* 8: 1376–1390.
- Vautard R, Thais F, Tobin I, Bréon FM, de Lavergne JGD, Colette A, Pascal Y, and Ruti PM (2014) Regional climate model simulations indicate limited climatic impacts by operational and planned European wind farms. *Nature Communications* 5: 3196.
- Veers P, Dykes K, Lantz E, Barth S, Bottasso CL, Carlson O, Clifton A, Green J, Green P, Holttinen H, Laird D, Lehtomäki V, Lundquist JK, Manwell J, Marquis M, Meneveau C, Moriarty P, Munduate X, Muskulus M, Naughton J, Pao L, Paquette J, Peinke J, Robertson A, Rodrigo JS, Sempreviva AM, Smith JC, Tuohy A, and Wiser R (2019) Grand challenges in the science of wind energy. *Science* 366: 6464.
- Vermeer LJ, Sorensen JN, and Crespo A (2003) Wind turbine wake aerodynamics. *Progress in Aerospace Science* 39: 467–510.
- Volker PJH, Badger J, Hahmann AN, and Ott S (2015) The explicit wake parametrisation V1.0: A wind farm parametrisation in the mesoscale model WRF. *Geoscientific Model Development* 8: 3481–3522.
- Walsh-Thomas JM, Cervone G, Agouris P, and Manca G (2012) Further evidence of impacts of large-scale wind farms on land surface temperature. *Renewable and Sustainable Energy Reviews* 16: 6432–6437.
- Wan Z (2006) New refinements and validation of the MODIS land surface temperature/emissivity products. *Remote Sensing of Environment* 112: 59–74.
- Wang C and Prinn RG (2010) Potential climatic impacts and reliability of very large-scale wind farms Atmos. *Chemical Physics* 10: 2053–2061.
- Wang C and Prinn RG (2011) Potential climatic impacts and reliability of large-scale offshore wind farms. *Environmental Research Letters* 6: 025101.
- Wang J, Yan Z, Jones PD, and Xia J (2013) On “observation minus reanalysis” method: A view from multi decadal variability. *Journal of Geophysical Research – Atmospheres* 118: 7450–7458.
- WindEurope (2017) *Wind in Power 2017. Annual Combined Onshore and Offshore Wind Energy Statistics*. Published February 2018. <https://windeurope.org/about-wind/statistics/european/wind-in-power-2017/>.
- Wiser R, Yang Z, Hand M, Hohmeyer O, Infield D, Jensen PH, Nikolaev V, O'Malley M, Sinden G, and Zervos A (2011) Wind energy. In: Edenhofer O, Pichs-Madruga R, Sokona Y, Seyboth K, Matschoss P, Kadner S, ... von Stechow C (eds.) *IPCC Special Report on Renewable Energy Sources and Climate Change Mitigation*. Cambridge, United Kingdom and New York, NY, USA: Cambridge University Press.
- United Nations (UN) (2019) *World Population Prospects 2019: Highlights*. 46. ISBN: 978-92-1-148316-1, New York, 2019.
- Xia G and Zhou L (2017) Detecting wind farm impacts on local vegetation growth in Texas and Illinois using MODIS vegetation greenness measurements. *Remote Sensing* 9: 698.
- Xia G, Zhou L, Freedman J, and Baidya Roy S (2016) A case study of effects of atmospheric boundary layer turbulence, wind speed, and stability on wind farm induced temperature changes using observations from a field. *Climate Dynamics* 46: 2179–2196.
- Xia G, Cervarich M, Baidya Roy S, Zhou L, Minder J, Freedman JM, and Jiménez PA (2017) Simulating impacts of real-world wind farms on land surface temperature using WRF model: Validation with MODIS observations. *Monthly Weather Review* 145: 4813–4836.

- Xia G, Zhou L, Minder JR, Fovell RG, and Jimenez PA (2019) Simulating impacts of real-world wind farms on land surface temperature using the WRF model: Physical mechanisms. *Climate Dynamics* 53: 1723–1739.
- Xu K, He L, Hu H, Liu S, Du Y, Wang Z, and Wang G (2019) Positive ecological effects of wind farms on vegetation in China's Gobi Desert. *Scientific Reports* 9: 1–11.
- Yeager K, Dayo F, Fisher B, Fouquet F, Gilau A, and Rogner HH (2012) Energy and economy. In: *Global Energy Assessment—Toward a Sustainable Future*, pp. 385–422. Cambridge (UK) and New York (USA)/Laxenburg (Austria): Cambridge University Press/International Institute for Applied Systems Analysis.
- Zhang W, Markfort CD, and Porté-Agel F (2013) Experimental study of the impact of large-scale wind farms on land-atmosphere exchanges. *Environmental Research Letters* 8: 1–9.
- Zhang X, Yang C, and Li S (2019) Influence of the heights of low-level jets on power and aerodynamic loads of a horizontal axis wind turbine rotor. *Atmosphere* 10: 132.
- Zhou L, Dickinson RE, Tian Y, Fang J, Li Q, Kaufmann RK, Tucker CJ, and Myneni RB (2004) Evidence for a significant urbanization effect on climate in China. *Proceedings of the National Academy of Sciences of the United States of America* 101: 9540–9544.
- Zhou L, Tian Y, Baidya Roy S, Thorncroft C, Bosart LF, and Hu Y (2012) Impacts of wind farms on land surface temperature. *Nature Climate Change* 2: 539–543.
- Zhou L, Tian Y, Baidya Roy S, Dai Y, and Chen H (2013a) Diurnal and seasonal variations of wind farm impacts on land surface temperature over Western Texas. *Climate Dynamics* 41: 307–326.
- Zhou L, Tian Y, Chen H, Dai Y, and Harris RA (2013b) Effects of topography on assessing wind farm impacts using MODIS data. *Earth Interactions* 17: 1–18.
- Zhou L, Tian Y, Myneni RB, Ciais P, Saathi S, Liu YY, Piao SL, Chen HS, Vermote EF, Song CH, and Hwang TH (2014) Widespread decline of Congo rainforest greenness in the past decade. *Nature* 509: 86–90.